Naval Research Laboratory

Washington, DC 20375-5000

NRL Memorandum Report 6411

Calculation of the Odd and Even Integral Components of the Wave Resistance Green's Function

HENRY T. WANG

Center for Fluid/Structure Interactions
Laboratory for Computational Physics and Fluid Dynamics

JOEL C.W. ROGERS

Department of Mathematics
Polytechnic Institute of New York

September 5, 1989

SECURITY CLASSIFICATION OF THIS PAGE

REPORT DOCUMENTATION PAGE

Form Approved
OMB No 0704-0188

1a REPORT SECURITY CLASSIFICATION UNCLASSIFIED	1b RESTRICTIVE MARKINGS
2a SECURITY CLASSIFICATION AUTHORITY	3 DISTRIBUTION / AVAILABILITY OF REPORT Approved for public release; distribution unlimited.
2b DECLASSIFICATION / DOWNGRADING SCHEDULE	
4 PERFORMING ORGANIZATION REPORT NUMBER(S) NRL Memorandum Report 6411	5 MONITORING ORGANIZATION REPORT NUMBER(S)
6a NAME OF PERFORMING ORGANIZATION Naval Research Laboratory 6b OFFICE SYMBOL (If applicable) Code 4420	7a NAME OF MONITORING ORGANIZATION
6c ADDRESS (City, State, and ZIP Code) Washington, DC 20375-5000	7b ADDRESS (City, State, and ZIP Code)
8a NAME OF FUNDING / SPONSORING ORGANIZATION Office of Naval Research 8b OFFICE SYMBOL (If applicable)	9 PROCUREMENT INSTRUMENT IDENTIFICATION NUMBER
8c ADDRESS (City, State, and ZIP Code) Arlington, VA 22217	10 SOURCE OF FUNDING NUMBERS PROGRAM ELEMENT NO: 61153N; PROJECT NO:; TASK NO: RR023-01-41; WORK UNIT ACCESSION NO: DN158-017

11 TITLE (Include Security Classification)
Calculation of the Odd and Even Integral Components of the Wave Resistance Green's Function

12 PERSONAL AUTHOR(S)
Wang, H.T. and Rogers, J.C.W.

13a TYPE OF REPORT	13b TIME COVERED	14 DATE OF REPORT (Year, Month, Day)	15 PAGE COUNT
Interim	FROM 6/87 TO 4/89	1989 September 5	42

16 SUPPLEMENTARY NOTATION

17 COSATI CODES			18 SUBJECT TERMS (Continue on reverse if necessary and identify by block number)
FIELD	GROUP	SUB-GROUP	Wave resistance Green's function; Computer code Odd and even components; Robust method Real single integrals

19 ABSTRACT (Continue on reverse if necessary and identify by block number)

This report presents a computerized method for calculating the total Green's function for the wave resistance case of a source in steady translation below the free surface. Starting with a representation of this function in the complex plane given by Bessho a series of transformations of variables are used to reduce it to three real single integrals. The integrands are regular and are entirely in terms of elementary functions. Two of the integrals are even about x=0 while the remaining integral is odd. The even and odd integrals may also be conveniently expressed in terms of the near and far field components. The method is robust, except for the well known difficulties at the limiting cases when the source is located near the free surface, or the field point is close to the source.

(Continues)

20 DISTRIBUTION / AVAILABILITY OF ABSTRACT	21 ABSTRACT SECURITY CLASSIFICATION
☒ UNCLASSIFIED/UNLIMITED ☐ SAME AS RPT ☐ DTIC USERS	UNCLASSIFIED

22a NAME OF RESPONSIBLE INDIVIDUAL	22b TELEPHONE (Include Area Code)	22c OFFICE SYMBOL
Henry T. Wang	(202) 767-2516	Code 4420

DD Form 1473, JUN 86 — Previous editions are obsolete. — SECURITY CLASSIFICATION OF THIS PAGE

S/N 0102-LF-014-6603

19. ABSTRACTS (Continued)

A computer code has been written to implement the above method. Sample calculated results are given in several forms to illustrate usage, accuracy, and computer time requirements of the code, as well as to show the relative behavior of the component integrals.

CONTENTS

CALCULATION OF THE ODD AND EVEN INTEGRAL COMPONENTS OF THE WAVE RESISTANCE GREEN'S FUNCTION

I. INTRODUCTION

For a number of decades, interest in the important Green's function for a submerged nonoscillating source moving at constant forward speed in fluid of infinite depth has largely centered on its far field characteristics. This was both due to the greater simplicity of the far field evaluation as well as its direct applicability to finding the hull resistance component due to wavemaking. The far field wave pattern required only the evaluation of a single integral with a regular integrand over a one-dimensional wavenumber space while the complete Green's function involves the additional calculation of a double integral with a singular integrand over a two-dimensional wavenumber space. The applicability of using only the far field analysis to obtain the wave resistance was aided by the pioneering work of Michell [1] who showed that reasonable estimates of the source strengths modeling the hull surface for the case of thin ships could be obtained directly from ship geometry, without need to ascertain the near field mutual influence of the sources. The landmark paper by Eggers, Sharma, and Ward [2] presents a comprehensive survey of different methods of using the single-integral far field Green's function to obtain the wave resistance.

In recent years, with the availability of ever faster computers and the design of fuller hulls, such as container ships, interest has been enlarged to include the near field terms of the Green's function. Such an evaluation would give a more accurate determination of the source strengths for hull forms which do not conform to thin ship theory as well as a more detailed definition of the flow field and pressure forces on or near the hull. Efforts aimed at rendering the near field part (or entire Green's function) amenable to numerical calculation usually involve expressing the additional double integral as a series of single integrals [3,4]. However, the integrands of the near field integrals are in terms of the exponential integral function. While this function is well known and series expansions are readily available [5], it is nevertheless defined by an integral expression and must be considered to be a higher order derived function.

By means of a series of ingenious transformations, Bessho [6] succeeds in reducing the entire Green's function to a single integral along a curved path in the complex plane. The integrand is regular and involves only elementary functions. Ursell [7] gives a more complete derivation of Bessho's remarkable result and justifies an important intermediate step. This report presents a numerical implementation of Bessho's work.

The report starts with a concise statement of the critical points of Bessho's contribution. Then, a more complete description of the derivation is given in outline form. The numerical implementation of the method is described next. This consists of a number of transformations and changes of path of integration required to reduce the original complex integrals to three real integrals. A brief description is given of the simple FORTRAN 77 computer program KELGREEN and its computer time

Manuscript approved March 30, 1989.

requirements. Some numerical results are presented to check on the accuracy of the procedure and to illustrate in graphical form the behavior of the calculated component integrals of the entire Green's function. The report concludes with a summary of the principal findings.

2. DERIVATION OF BESSHO'S SINGLE INTEGRAL REPRESENTATION

2.1 Initial Representation in Double Integral Form

In this work, we will consistently follow the notation used by Ursell [7]. Figure 1 shows the coordinate system used in our work, where x corresponds to the direction of the current flow U, y is the horizontal direction perpendicular to x, and z is the vertical direction positive downwards. For a stationary nonoscillating source located at (X,Y,Z) the Green's function $G(x,y,z\,;\,X,Y,Z)$ is given by

$$G(x,y,z) = \frac{1}{R^1} - \frac{1}{R} + G_0 \tag{1}$$

where

$$R^1 = [(x-X)^2 + (y-Y)^2 + (z-Z)^2]^{1/2}$$

$$R = [(x-X)^2 + (y-Y)^2 + (z+Z)^2]^{1/2}$$

$$G_0 = \frac{-1}{\pi} \lim_{\epsilon \to 0} \int_{-\pi}^{\pi} d\theta \int_0^{\infty} dk \, \frac{\exp\,[-k(z+Z) + ik\,(x - X)\cos\theta + ik(y - Y)\sin\theta]}{k\cos^2\theta - 1 - i\epsilon\cos\theta} \tag{2}$$

In the above equation, all length variables have been made dimensionless by multiplication by the factor g/U^2 where g is the gravity constant. G_0 represents an inverse double Fourier transform over the two-dimensional $k-\theta$ wavenumber space. Also, following Ursell, the terms $(x - X)$, $(y - Y)$, and $(z + Z)$ appearing in Eq. (2) are simply replaced by x,y, and z for the sake of convenience. This is equivalent to taking the source to be located at the origin (0,0,0).

2.2 Concise Statement of Bessho's Approach

The usual way of simplifying the double integral expression for G_0 is to perform an initial integration over k or θ, thus reducing the double integral to a single integral. The integrand, however, is not entirely in terms of elementary functions but contains the higher order derived exponential integral function $E_1(u)$ defined by

$$E_1(u) = \int_u^{\infty} \frac{e^{-\lambda}}{\lambda}\, d\lambda \tag{3}$$

In Bessho's approach, the initial integration to reduce the double integral to a single integral is not performed at the outset. Instead, after a series of transformations of the double integral, including changes of variables, deformation of the paths of integration in the complex plane, expressing G_0 as derivatives of more convergent integrals, and interchanging order of integration, the double integral is finally converted to single integral form by means of the following crucial equality

$$\int_{-\infty}^{\infty} \frac{\exp\,(i\,m\,P)}{m - Q}\, dm = \begin{cases} 2\pi i \exp\,(i\,P\,Q) & (P > 0,\ \mathrm{Im}\,Q > 0) \\ -2\pi i \exp\,(i\,P\,Q) & (P < 0,\ \mathrm{Im}\,Q < 0) \\ 0 & (P \cdot \mathrm{Im}\,Q < 0) \end{cases} \tag{4}$$

where P is real and Q is complex. Thus, the order of integration is reduced entirely in terms of elementary functions. The following section gives a more complete summary of Ursell's detailed derivation and justification of Bessho's approach.

2.3 Summary of Ursell's Derivation

Using the equaiity

$$\int_{\pi/2}^{\pi} \cos\theta \, d\theta = \int_{0}^{\pi/2} -\cos\theta \, d\theta \tag{5}$$

rewrite G_0 in Eq. (2) as the foilowing sum of A and B

$$G_0(x,y,z) = A(x,y,z) + B(x,y,z) \tag{6}$$

$$A(x,y,z) = \frac{-1}{\pi} \lim_{\epsilon \to 0} \int_{-\pi/2}^{\pi/2} d\theta \int_{0}^{\infty} dk \; \frac{\exp(-kz + ikx\cos\theta + iky\sin\theta)}{k\cos^2\theta - 1 - i\epsilon\cos\theta} \tag{7a}$$

$$B(x,y,z) = \frac{-1}{\pi} \lim_{\epsilon \to 0} \int_{-\pi/2}^{\pi/2} d\theta \int_{0}^{\infty} dk \; \frac{\exp(-kz - ikx\cos\theta + iky\sin\theta)}{k\cos^2\theta - 1 + i\epsilon\cos\theta} \tag{7b}$$

By introducing the following two sets of new variables

$$m = k\cos\theta, \quad \tanh\nu = \sin\theta \tag{8a}$$

$$y = \rho\sin\alpha, \quad z = \rho\cos\alpha, \quad x = \rho\sinh\beta, \quad R = \rho\cosh\beta \tag{8b}$$

and writing A and B as

$$A = A_0 + i\frac{\partial}{\partial x} A_1 \tag{9a}$$

$$B = B_0 + i\frac{\partial}{\partial x} B_1 \tag{9b}$$

the following expressions are obtained for A_0, B_0, A_1, and B_1,

$$A_0 = \frac{1}{\pi} \int_{0}^{\infty} dm \int_{-\infty}^{\infty} d\nu \exp[-m\rho\cosh(\nu - i\alpha) + imx] \tag{10a}$$

$$B_0 = \frac{1}{\pi} \int_{0}^{\infty} dm \int_{-\infty}^{\infty} d\nu \exp[-m\rho\cosh(\nu - i\alpha) - imx] \tag{10b}$$

$$A_1 = \frac{1}{\pi} \lim_{\epsilon \to 0} \int_{0}^{\infty} dm \int_{-\infty}^{\infty} d\nu \; \frac{\exp[-m\rho\cosh(\nu - i\alpha) + imx]}{m - \cosh\nu - i\epsilon} \tag{10c}$$

$$B_1 = \frac{-1}{\pi} \lim_{\epsilon \to 0} \int_{0}^{\infty} dm \int_{-\infty}^{\infty} d\nu \; \frac{\exp[-m\rho\cosh(\nu - i\alpha) - imx]}{m - \cosh\nu + i\epsilon} \tag{10d}$$

The reason for introducing the new integrals A_1 and B_1 is that they are more strongly convergent than the original integrals A and B.

The double integrals A_0 and B_0 are simplified by Ursell by making the change of variables $v - i\alpha \to v$, and using equality (9.6.24) of Ref. [5] to convert the integrand in terms of the Bessel function K_0

$$A_0 + B_0 = \frac{1}{\pi}\int_0^\infty dm \int_{-\infty+i\alpha}^{\infty+i\alpha} dv \exp[-m\rho \cosh(v - i\alpha)] [\exp(imx) + \exp(-imx)]$$

$$= \frac{4}{\pi}\int_0^\infty dm\, K_0(m\rho)\cos mx = \frac{2}{\sqrt{\rho^2 + +x^2}} = \frac{2}{R} \tag{11a}$$

Actually, the integral $A_0 + B_0$ can be more directly simplified (without the need to use Bessel functions) by noting that the order of integration can be interchanged since it is absolutely convergent, carrying out the simple integral with respect to m, and making the change of variables $w = e^v$ in the resulting single integral to arrive at the same result given above

$$A_0 + B_0 = \frac{1}{\pi}\int_{-\infty}^{\infty} dv \left(\frac{1}{\rho\cosh v - ix} + \frac{1}{\rho\cosh v + ix}\right)$$

$$= \frac{1}{\pi}\int_0^w dw \left(\frac{1}{\frac{\rho}{2}w^2 + ixw + \frac{\rho}{2}} + \frac{1}{\frac{\rho}{2}w^2 - ixw + \frac{\rho}{2}}\right)$$

$$= \frac{2}{\pi\sqrt{\rho^2 + x^2}}\left(\frac{\pi}{2} + \frac{\pi}{2}\right) = \frac{2}{\sqrt{\rho^2 + x^2}} = \frac{2}{R} \tag{11b}$$

By making similar shifts in the paths of integration of A_1 ($v = i\alpha + \frac{1}{2}\pi i + w$, w real) and B_1 ($v = i\alpha - \frac{1}{2}\pi i + w$, w real), the sum $A_1 + B_1$ takes the form

$$A_1 + B_1 = \frac{1}{\pi}\lim_{\epsilon\to 0}\int_{-\infty}^{\infty} dm \int_{-\infty}^{\infty} dw\, \frac{\exp(-im\rho\sinh w + im\rho\sinh\beta)}{m - i\sinh(w + i\alpha) - i\epsilon}$$

$$+ \text{(single integrals due to residues at poles crossed by the shifts)} \tag{12}$$

By interchanging the order of integration, Bessho notes that the integral with respect to m is of the form given in Eq. (4) and thus the double integral is converted to a single integral entirely in terms of elementary functions.

Ursell points out that the double integral in Eq. (12) does not satisfy the sufficient (but not necessary) condition of absolute convergence in order to justify the interchange of order of integration. His proof of the validity of the interchange basically consists of extending Bessho's idea of generating derivative functions, shown in Eq. (9), to generate the following still more strongly convergent integrals A_2 and B_2

$$A_2 = \frac{1}{\pi} \lim_{\epsilon \to 0} \int_0^\infty dm \int_{-\infty}^\infty dv \, \frac{\exp\left[-m\rho \cosh(v - i\alpha) + imx\right]}{(1 - i)(m - \cosh v - i\epsilon)} \tag{13a}$$

$$B_2 = \frac{-1}{\pi} \lim_{\epsilon \to 0} \int_0^\infty dm \int_{-\infty}^\infty dv \, \frac{\exp\left[-m\rho \cosh(v - i\alpha) - imx\right]}{(1 + im)(m - \cosh v + i\epsilon)} \tag{13b}$$

which are related to A_1 and B_1 as follows

$$A_1 = \left(1 - \frac{\partial}{\partial x}\right) A_2 \tag{14a}$$

$$B_1 = \left(1 - \frac{\partial}{\partial x}\right) B_2 \tag{14b}$$

Ursell proceeds to operate on A_2 and B_2 in a manner similar to Bessho's transformations of A_1 and B_1. That is, once again the paths of integration are shifted for A_2 ($v = i\alpha + \frac{1}{2}\pi i + w$, w real) and B_2($v = i\alpha - \frac{1}{2}\pi i + w$, w real), and the resultant residue evaluated at the pole of the integrand crossed by this shift (for some but not all m) where the pole V is defined by

$$\cosh V(m) = \begin{cases} m + i\epsilon & \text{for } B_2 \\ m - i\epsilon & \text{for } A_2 \end{cases} \tag{15}$$

By making the further change of variables from m to V, as given in Eq. (15), in the single integral resulting from the residue evaluation, the following expressions are obtained for A_2 and B_2, where each is given in terms of a single integral and a double integral

$$A_2 = \frac{1}{\pi} \lim_{\epsilon \to 0} \int_0^\infty \frac{dm}{1 - im} \int_{-\infty}^\infty dw \, \frac{\exp(-im\rho \sinh w + im\rho \sinh \beta)}{m - i \sinh(w + i\alpha) - i\epsilon} \tag{16a}$$

$$-2i \int_{\frac{1}{2}\pi i}^{-\infty} dv \, \frac{\exp(-\rho \cosh V \cosh(V - i\alpha) + ix \cosh V)}{1 - i \cosh V} \tag{16b}$$

$$B_2 = \frac{-1}{\pi} \lim_{\epsilon \to 0} \int_0^\infty \frac{dm}{1 + im} \int_{-\infty}^\infty dw \, \frac{\exp(im\rho \sinh w - im\rho \sinh \beta)}{m + i \sinh(w + i\alpha) + i\epsilon} \tag{16c}$$

$$-2i \int_{i(\alpha - \frac{1}{2}\pi)}^{-\infty} dV \, \frac{\exp(-\rho \cosh V \cosh(V - i\alpha) - ix \cosh V)}{1 + i \cosh V} \tag{16d}$$

where α is taken to be ≥ 0 in Eqs. (16b) and (16d).

Ursell shows that the double integrals (16a) and (16c) are absolutely convergent, and thus it is permissible to interchange the order of integration. By writing $-m$ for m in Eq. (16c) the two double integrals can be combined into a single form, with order of integration interchanged

Eq. (16a) + Eq. (16c)

$$= \frac{1}{\pi}\int_{-\infty}^{\infty} dw \int_{-\infty}^{\infty} dm \; \frac{\exp\left(-im\rho \sinh w + im\rho \sinh \beta\right)}{(1 - im)\,[m - i \sinh (w + i\alpha)]}$$

$$= \frac{1}{\pi}\int_{-\infty}^{\infty} dw\, I(w, \beta) \tag{17a}$$

The presence of the extra factor $(1 - im)$ in the denominator makes the equalities given by Eq. (4) not directly applicable for evaluating $I(w, \beta)$. Instead, Ursell evaluates it by means of an elaborate contour integration, accounting for the residues due to the poles which are enclosed for $0 < w < \beta$ and $\beta < w < \infty$. Actually, Eq. (17a) can be put in a form to which Eq. (4) is applicable, by rewriting the denominator, as follows

$$\frac{1}{(1 - im)[m - i \sinh(w + i\alpha)]} = \frac{1}{\sinh(w + i\alpha) + 1}\left[\frac{1}{m - i \sinh (w + i\alpha) - \dfrac{1}{m + i}}\right] \tag{17b}$$

In either case, Eq. (17a) is expressed as the following sum of two single integrals

$$\frac{1}{\pi}\int_{-\infty}^{\infty} I(w, \beta) dw = 2i \int_{0}^{\beta} \frac{\exp\left[-\rho\,(\sinh \beta - \sinh w) \sinh\,(w + i\alpha)\right]}{1 + \sinh\,(w + i\alpha)}\, dw \tag{18a}$$

$$+ 2i \int_{\beta}^{\infty} \frac{\exp\left[\rho(\sinh\beta - \sinh w)\right]}{1 + \sinh\,(w + i\alpha)}\, dw \tag{18b}$$

The component single integrals (16b), (16d), (18a), and (18b) which together define $A_2 + B_2$ form the starting point for our numerical analysis and implementation. We will, however, complete Ursell's derivation in which he essentially sums these component integrals and performs the derivatives indicated in Eqs. (14) and (9) to obtain Bessho's representation of $G_0 = A + B$ as a single integral in the complex plane.

To begin the compacting process, these four integrals are all expressed in terms of the variable u by letting $V = u + \frac{1}{2}\pi i$ in Eq. (16b), $V = u - \frac{1}{2}\pi i$ in Eq. (16d), and $w = u - i\alpha$ in Eqs. (18a) and (18b), resulting in

$$A_2 + B_2 = 2i \left[\int_{-\infty + \frac{1}{2}\pi i}^{\beta + i\alpha} + \int_{-\infty - \frac{1}{2}\pi i}^{0}\right] \frac{du}{1 + \sinh u} \exp\left[(\rho \sinh\,(u - i\alpha) - x) \sinh u\right]$$

$$+2i \int_{\beta + i\alpha}^{\infty + i\alpha} \frac{du}{1 + \sinh u} \exp\left[-(\rho \sinh\,(u - i\alpha) - x)\right] \tag{19}$$

In carrying out the differentiations $\partial/\partial x$ indicated in Eqs. (14) and (9) it is important to recognize that the limits of integration involve the variables α and β. From the transformation Eq. (8b), it is seen that

$$\frac{\partial \alpha}{\partial x} = 0, \quad 1 = \rho \cosh \beta \frac{\partial \beta}{\partial x} \rightarrow \frac{\partial \beta}{\partial x} = \frac{1}{R} \tag{20}$$

Performing the operations indicated in Eq. (14) on $A_2 + B_2$ yields the following integral representation for $A_1 + B_1$

$$A_1 + B_1 = (1 - \frac{\partial}{\partial x})(A_2 + B_2)$$

$$= 2i \left[\int_{-\infty+\frac{1}{2}\pi i}^{\beta+i\alpha} + \int_{-\infty-\frac{1}{2}\pi i}^{0} \right] \exp[(\rho \sinh(u - i\alpha) - x) \sinh u \, du] \quad (21)$$

Similarly, performing the transformation indicated by Eq. (9), using the result given in Eq. (11), and rearranging the limits of integration, the following complex single integral representation for G_0 is obtained

$$G_0 = A + B = \frac{2}{R} + i \frac{\partial}{\partial x}(A_1 + B_1)$$

$$= 2 \left[\int_{-\infty-\frac{1}{2}\pi i}^{\beta+i\alpha} + \int_{-\infty+\frac{1}{2}\pi i}^{0} \right] \sinh u \exp[(\rho \sinh(u - i\alpha) - x) \sinh u] \, du \quad (22)$$

The above integration paths are not the same as those used by Bessho, shown in Fig. 2. In order to obtain the integrals in the Bessho form, make the substitution $x = -X$, $X = \rho \sinh b$, $u = -v$, and note that $G_0(\alpha) = G_0(-\alpha)$, resulting in

$$G_0(-X,y,z) = -2 \left[\int_0^{\infty-\frac{1}{2}\pi i} + \int_{b+i\alpha}^{\infty+\frac{1}{2}\pi i} \right] \sinh v \exp[(\rho \sinh(v - i\alpha) - X) \sinh v] \, dv \quad (23)$$

3. COMPUTATIONAL IMPLEMENTATION OF BESSHO'S METHOD

In this chapter we will present our computational implementation of Bessho's method. As mentioned previously, our analysis starts from the 4 component complex single integrals given in Eqs. (16b), (16d), (18a), and (18b). Through a series of transformations, we simplify and condense these complex integrals to three real integrals, two of which are even in x and the other is odd in x. Taken together, these integrals represent the entire Green's function. A description is also given of the simple FORTRAN 77 computer program KELGREEN which evaluates these integrals. The description includes the structure of the program, input and output, and computer time requirements.

3.1 Simplification of Complex Integrals

We start by making the change of variables $\zeta = iV$ for part of the integration of Eqs. (16b) and (16d) and then rewrite each integral as two integrals with real limits of integration, resulting in the following expression for $A_2 + B_2$

$$A_2 + B_2 = 2i \int_0^{\beta} \frac{\exp[-\rho(\sinh\beta - \sinh w)\sinh(w + i\alpha)]}{1 + \sinh(w + i\alpha)} \, dw \quad (18a)$$

$$+ 2i \int_{\beta}^{\infty} \frac{\exp[\rho(\sinh\beta - \sinh w)]}{1 + \sinh(w + i\alpha)} \, dw \quad (18b)$$

$$- 2 \int_0^{\frac{1}{2}\pi} \frac{\exp\left[-\rho \cos \zeta \cos (\zeta - \alpha) + ix \cos \zeta\right]}{1 - i \cos \zeta} d\zeta \tag{16b.1}$$

$$+ 2i \int_{-\infty}^{0} \frac{\exp\left[-\rho \cosh V \cosh (V - i\alpha) + ix \cosh V\right]}{1 - i \cosh V} dV \tag{16b.2}$$

$$+ 2 \int_0^{\frac{\pi}{2}-\alpha} \frac{\exp\left[-\rho \cos \zeta \cos(\zeta + \alpha) - ix \cos \zeta\right]}{1 + i \cos \zeta} d\zeta \tag{16d.1}$$

$$+ 2i \int_{-\infty}^{0} \frac{\exp\left[-\rho \cosh V \cosh (V - i\alpha) - ix \cosh V\right]}{1 + i \cosh V} dV \tag{16d.2}$$

In the above, use has been made of the following identity relating trigonometric and hyperbolic cosines

$$\cosh (iV) = \cos V \tag{24}$$

Carrying out the differentiations indicated in Eq. (14), the following integrals are obtained for $A_1 + B_1$

$$A_1 + B_1 = (1 - \frac{\partial}{\partial x}) (A_2 + B_2)$$

$$= 2i \int_0^{\beta} \exp\left[-\rho(\sinh \beta - \sinh w) \sinh (w + i\alpha)\right] dw \tag{25a}$$

$$- 2 \int_0^{\frac{1}{2}\pi} \exp\left[-\rho \cos \zeta \cos (\zeta - \alpha) + ix \cos \zeta\right] d\zeta \tag{25b}$$

$$+ 2i \int_{-\infty}^{0} \exp\left[-\rho \cosh V \cosh (V - i\alpha) + ix \cosh V\right] dV \tag{25c}$$

$$+ 2 \int_0^{\frac{\pi}{2}-\alpha} \exp\left[-\rho \cos \zeta \cos (\zeta + \alpha) - ix \cos \zeta\right] d\zeta \tag{25d}$$

$$+ 2i \int_{-\infty}^{0} \exp\left[-\rho \cosh V \cosh (V - i\alpha) - ix \cosh V\right] dV \tag{25e}$$

The above equation is a result of the following considerations. Recalling from Eq. (20) that $\partial\beta/\partial x = 1/R$, the derivatives $\partial/\partial x$ of the variable limits of integration appearing in Eqs. (18a) and (18b) cancel each other. Recalling from Eq. (8b) that $x = \rho \sinh \beta$ the operation $(1 - \partial/\partial x)$ applied to the integrands results in Eq. (18b) going to zero and a removal of the denominator in the other five integrals.

Proceeding similarly, using Eqs. (9) and (11), we obtain G_0 in the form

$$G_0 = A + B = \frac{2}{R} + i \frac{\partial}{\partial x} (A_1 + B_1)' = G_1 + G_2 + G_3 + G_4$$

$$= 2 \int_0^{\beta} \sinh (w + i\alpha) \exp [-\rho(\sinh \beta - \sinh w) \sinh (w + i\alpha)] \, dw \tag{26a}$$

$$+ 2 \int_0^{\frac{1}{2}\pi} \cos \zeta \exp[-\rho \cos \zeta \cos (\zeta - \alpha) + ix \cos \zeta] \, d\zeta \tag{26b}$$

$$+ 2 \int_0^{\frac{\pi}{2}-\alpha} \cos \zeta \exp [-\rho \cos \zeta \cos (\zeta + \alpha) - ix \cos \zeta] \, d\zeta \tag{26c}$$

$$+ 4 \int_{-\infty}^{0} \cosh V \sin (x \cosh V) \exp [-\rho \cosh V \cosh (V - i\alpha)] \, dV \tag{26d}$$

In the above equation, the two integrals in terms of the variable V have been combined into a single integral by using the well known identity

$$e^{ix \cosh V} - e^{-ix \cosh V} = 2i \sin (x \cosh V) \tag{27}$$

In the following, we express the above complex integrals as the sum of real and imaginary parts, and consider only the real part. By means of a series of transformations, we reduce the resulting integrals to compact form.

3.2 Conversion to Real Integrals

Consider first G_1 given by Eq. (26a). By making use of the equality

$$\sinh (w + i\alpha) = \sinh w \cosh(i\alpha) + \cosh w \sinh(i\alpha)$$

$$= \sinh w \cos \alpha + i \cosh w \sin \alpha \tag{28}$$

G_1 is expressed as the following integral with a two-term integrand

$$G_1 = 2 \int_0^{\beta} [\sinh w \cos \alpha \cos [\rho(\sinh \beta - \sinh w) \cosh w \sin \alpha]$$

$$+ \sinh w \sin \alpha \sin [\rho(\sinh \beta - \sinh w) \cosh w \sin \alpha]] \times$$

$$\exp [-\rho \sinh \beta - \sinh w) \sinh w \cos \alpha] \, dw \tag{29}$$

By making the change of variables $\cosh w\, dw = dw'$ and making use of the hyperbolic identity $\sinh^2 w = \cosh^2 w - 1$, G_1 becomes the following

$$G_1 = 2\int_0^{\sinh\beta = x/\rho} [\cos\alpha \frac{w}{\sqrt{w^2+1}} \cos(x \sin\alpha \sqrt{w^2+1} - yw\sqrt{w^2+1})$$

$$+ \sin\alpha \sin(x \sin\alpha \sqrt{w^2+1} - yw\sqrt{w^2+1})]\, e^{-x\cos\alpha\, w + zw^2}\, dw \qquad (30)$$

Let us now consider G_2 and G_3 given by Eqs. (26b) and (26c). By using the well known relationship $e^{\pm ix\cos\zeta} = \cos(x\cos\zeta) \pm i \sin(x\cos\zeta)$, the real part of these two integrals can be conveniently written out. By making the change of variables $\zeta = -\zeta'$ in G_3, $G_2 + G_3$ can be written as the following single integral

$$G_2 + G_3 = 2\int_{\frac{-\pi}{2}+\alpha}^{\frac{1}{2}\pi} \cos\zeta \cos(x\cos\zeta) e^{-\rho\cos\zeta\cos(\zeta-\alpha)} d\zeta \qquad (31)$$

By making the change of variables $\zeta = \zeta' + \alpha/2$, and using various trigonometric identities for the cosine terms in the exponential, $G_2 + G_3$ take the following symmetric form with respect to the limits of integration

$$G_2 + G_3 = 2\int_{\frac{-\pi}{2}+\frac{\alpha}{2}}^{\frac{\pi}{2}-\frac{\alpha}{2}} \cos(\zeta + \frac{\alpha}{2}) \cos(x\cos(\zeta + \frac{\alpha}{2}))\, e^{\frac{-\rho}{2}(\cos 2\zeta + \cos\alpha)} d\zeta \qquad (32)$$

Expanding the cosine terms in front of the exponential, and keeping only the even functions of ζ (since the odd functions give a zero integral), $G_2 + G_3$ takes the form

$$G_2 + G_3 = 4\int_0^{\frac{\pi}{2}-\frac{\alpha}{2}} [\cos\zeta \cos\frac{\alpha}{2} \cos(x\cos\frac{\alpha}{2}\cos\zeta) \cos(x\sin\frac{\alpha}{2}\sin\zeta)$$

$$- \sin\zeta \sin\frac{\alpha}{2} \sin(x\cos\frac{\alpha}{2}\cos\zeta) \sin(x\sin\frac{\alpha}{2}\sin\zeta)] e^{\frac{-\rho}{2}(\cos 2\zeta + \cos\alpha)} d\zeta \qquad (33)$$

Very similar to the transformation indicated after Eq. (29), by making the change of variables $\cos\zeta d\zeta = dw$, $G_2 + G_3$ takes the following form of the sum of two integrands with common limits of integration

$$G_2 + G_3 = 4\int_0^{\cos\frac{\alpha}{2}} [\cos\frac{\alpha}{2} \cos(x\cos\frac{\alpha}{2}\sqrt{1-w^2}) \cos(x\sin\frac{\alpha}{2} w)$$

$$- w \frac{\sin\frac{\alpha}{2}}{\sqrt{1-w^2}} \sin(x\cos\frac{\alpha}{2}\sqrt{1-w^2}) \sin(x\sin\frac{\alpha}{2} w)] e^{\frac{-\rho}{2}(\cos\alpha + 1 - 2w^2)} dw \qquad (34)$$

Finally, let us consider G_4 given by Eq. (26d). By making use of the identity

$$\cosh (V - i\alpha) = \cosh V \cos \alpha - i \sinh V \sin \alpha \tag{35}$$

the real part of G_4 is written as

$$G_4 = 4 \int_0^\infty \cosh V \sin (x \cosh V) \cos (\rho \cosh V \sinh V \sin \alpha)\, e^{-\rho \cosh^2 V \cos \alpha}\, dV \tag{36}$$

By making the change of variables $\cosh V\, dV = dw$ and recalling Eq. (8b), G_4 becomes

$$G_4 = 4 \int_0^\infty \sin (x\sqrt{w^2 + 1}) \cos (yw\sqrt{w^2 + 1})e^{-z(w^2+1)}\, dw \tag{37}$$

By making the change of variables $dw = \sec^2\theta d\theta$, we can transform G_4 to the single integral form given in Eq. (13.3b) of Wehausen and Laitone [8]

$$G_4 = 4 \int_0^{\pi/2} \sin (x\sec^2\theta \cos \theta) \cos (y \sec^2\theta \sin \theta)e^{-z \sec^2\theta} \sec^2\theta d\theta \tag{38}$$

In our numerical computations we find it somewhat more convenient to make the change of variables $\sec^2\theta \sin \theta = u$ and use the following alternate form proposed in [2]

$$G_4 = 4 \int_0^\infty \sin (xs) \cos (yu)e^{-s^2 z} \frac{s}{2s^2 - 1} du \tag{39}$$

where $s(u) = \left[\dfrac{1 + \sqrt{1 + 4u^2}}{2}\right]^{1/2} = \sec \theta.$

Adding the component integrals given by Eqs. (30), (34), and (39), the resulting form for G_0 in real form is given by

$$G_0 = G_x + G_c + G_o = G_e + G_o$$

$$= 2 \int_{=0}^{x/\rho} \left[\cos \alpha \frac{w}{\sqrt{w^2 + 1}} \cos (x \sin \alpha \sqrt{w^2 + 1} - yw \sqrt{w^2 + 1})\right.$$

$$\left. + \sin \alpha \sin (x \sin \alpha \sqrt{w^2 + 1} - yw \sqrt{w^2 + 1})\right]e^{-x \cos \alpha w + \rho \cos \alpha w^2} dw \tag{40a}$$

$$+ 4 \int_0^{\cos \frac{\alpha}{2}} \left[\cos \frac{\alpha}{2} \cos (x \cos \frac{\alpha}{2} \sqrt{1 - w^2}) \cos (x \sin \frac{\alpha}{2} w)\right.$$

$$\left. \frac{-w \sin \frac{\alpha}{2}}{\sqrt{1 - w^2}} \sin (x \cos \frac{\alpha}{2} \sqrt{1 - w^2}) \sin (x \sin \frac{\alpha}{2} w)\right]e^{\frac{-\rho}{2}(\cos \alpha + 1 - 2w^2)} dw \tag{40b}$$

$$+ 4 \int_0^\infty \sin(xs) \cos(yu) e^{-s^2 z} \frac{s}{2s^2 - 1} du \tag{40c}$$

where $s(u)$ is defined in Eq. (39), and ρ and α in Eq. (8b). Since G_o given by Eq. (40c) corresponds to the single integral part of the total Green's function given in [8], G_e, the sum of G_x and G_c given respectively by Eqs. (40a) and (40b), corresponds to the double integral part. Eq. (40c) shows that G_o is odd about $x = 0$ and has an infinite upper limit of integration while Eqs. (40a) and (40b) show that the G_e is even about $x = 0$ and has finite upper limits of integration which depend on the field point. Thus, the even part is, on the whole, somewhat simpler to evaluate.

3.3 Numerical Integration Scheme

While the integrands of the three integrals in Eq. (40) are regular, there are the problems of the infinite upper limit in Eq. (40c) and the possible infinite upper limit in Eq. (40a) for $\rho \to 0$. These numerical difficulties are an indication of the well known nonuniform behavior of G_o in the neighborhood of the x-axis, $\rho = 0$. In the Appendix we have derived an expression giving the first order far field behavior of G_o in the neighborhood of $\rho = 0$. This expression generalizes, for the case of large x, the equation given by Euvrard [10] for the specialized case $z = 0$, $y = -0$. Since it is shown later in Eq. (45) that G_e differs from G_o by the near field component G_n, which is well behaved, G_e must then show a similar nonuniform behavior.

The error incurred by using a finite upper limit u_M in Eq. (40c) may be easily estimated by noting that the factor $\exp(-s^2 z)$ makes it a convergent integral for $z > 0$. By noting that the trigonometric factors always have magnitudes less or equal to 1, and changing the variable of integration to s defined in Eq. (39), the error ϵ is bounded as follows

$$\epsilon \leq 4 \int_{s_M}^\infty e^{-s^2 z} \frac{s^2}{u} ds \tag{41}$$

where $s_M^2 = \frac{1}{2} + \sqrt{\frac{1}{4} + u_M^2}$. By making the change of variables $t = s^2$, the above may be integrated by parts to give

$$\epsilon \leq \frac{2 e^{-s_M^2 z} s_M}{z u_M} + \frac{2}{z} \int_{s_M}^\infty e^{-s^2 z} \frac{d}{ds} \left(\frac{s}{u}\right) ds \tag{42}$$

where $\frac{d}{ds}\left(\frac{s}{u}\right) = \frac{d}{ds}(s^2 - 1)^{-1/2} \leq 0$. Therefore, it is necessary to consider only the first term in deriving estimates of the maximum error incurred by using finite values of u_M. By considering ϵ and z to be given parameters, Eq. (42) may be solved iteratively for the required upper limit u_M. Table 1 give the calculated values of u_M for ϵ = (0.01, 0.001, 0.0001) and z = (1.0, 0.3, 0.1, 0.03, 0.01, 0.003, 0.001). Table 1 shows the manner in which u_M increases with decreasing values of ϵ and z.

In the case of Eq. (40a), the neighborhood of $\rho = 0 (y = z = 0)$ leads to the upper limit of integration $x/\rho \to \infty$. The limiting value of the integral is, however, well behaved [9].

A simple trapezoidal rule and the higher order Simpson's rule are used to integrate each of the three integrals. Starting with an initial partition of the integration range into four intervals, the number of intervals is successively doubled until the integrated values from two successive iterations

agree to within a specified error criterion. In both Eqs. (40a) and (40c), where the arguments of the trigonometric functions may take on large values, the function AMOD is used to reduce the argument to the interval $(0,2\pi)$ to facilitate the evaluation of these functions. Also, advantage is taken of the nature of the argument of the exponential function in Eq. (40a), $f(w) = -x \cos\alpha\, w + \rho \cos\alpha\, w^2$, $0 \le w \le x/\rho$. It is easily seen that $f = 0$ at the ends of the interval, $w = 0$ and $w = x/\rho$, and takes on negative values in between. Thus, for the troublesome large x/ρ case, f may take on large negative values over most of the integration interval and the resulting small value of the factor e^f renders the contribution of the entire integrand negligible. In our approach, the integrand is not evaluated if f is less than a specified number, say, $f \le -20$.

3.4 Computer Program KELGREEN

The above numerical scheme has been implemented in the form of the FORTRAN 77 computer program KELGREEN. The program consists of a main program and the subroutines CPTIME and UNFORM. The main program reads input data, calculates the integrals in Eq. (40) for a rectangular $x - y$ grid of field points, and writes out the calculated results in formatted form. The subroutine CPTIME keeps track of the actual CPU time used for the calculations. The subroutine UNFORM writes onto an unformatted output file the dimensions of the $x - y$ grid, the CPU time used, and the calculated values of the integrals, in a form suitable for generating computer plots.

Input data are entered into the program by means of the two following READ statements.

```
      READ (5,521) filename
521   FORMAT (A30)
      READ (5,*) z, lcol, krow, x0, xdel, y0, ydel, umx, xpmx, erc, itm, ical, ipr
```

The input variables are defined as follows:

1. filename is the unformatted output file onto which are written the calculated values of the integrals.

2. z ($= \rho \cos\alpha$) is the submergence of the source below the free surface; this value is taken to be the same for all the field points.

3. lcol is the number of grid points in the x direction, $1 \le$ lcol ≤ 151.

4. krow is the number of grid points in the y direction, $1 \le$ krow ≤ 151.

5. x0 is the value of x for the initial grid point.

6. xdel is the value of Δx, the size of each grid cell in the x direction.

7. y0 is the value of y for the initial grid point.

8. ydel is the value of Δy, the size of each grid cell in the y direction.

9. umx is the upper limit of the integral in Eq. (40c); see Table 1.

10. xpmx is the maximum absolute value of the exponential factor f in Eq. (42a); for $|f| >$ xpmx, the rest of the integrand is not calculated; a value of 20 is recommended.

11. erc is the maximum permissible error ϵ in I_{n+1} and I_n, the calculated values of the integral for two successive iterations respectively using 2^{n+2} and 2^{n+1} integration intervals, where ϵ is defined as the absolute error $|I_{n+1} - I_n|$.

12. itm is the maximum number of integration iterations which are allowed; values of 20 to 30 are recommended.

13. ical is a calculation indicator such that for ical $\leq$ 1, the program calculates only the even integral part G_e given by Eqs. (40a) and (40b); for ical = 2, the program calculates all three integrals in Eq. (40); for ical $\geq$ 3, the program calculates only the odd integral part G_o given by Eq. (40c).

14. ipr is an output indicator such that for ipr $\geq$ 1, the calculated results are written onto a unformatted output file for later plotting; otherwise, this file is not generated; note that the formatted output given in the following section is always generated as standard output.

3.5 Sample Input and Output

Table 2 lists a sample input file and Table 3 lists the sample formatted output file resulting from this input file.

The first line of the output file lists the values of z and error criterion erc used for all the calculations, the value of umx to be used in Eq. (40c), and the value of xpmx to be used in Eq. (40a). The majority of the output is devoted to listing the following:

1. x, the x-location of the field point

2. y, the y-location of the field point

3. x/rh, x/ρ in Eq. (40a)

4. alfa, α in Eq. (40)

5. ix, the number of iterations required to calculate the integral in Eq. (40a); final number of integration intervals = 2^{ix+1}

6. ic, the number of iterations required to calculate the integral in Eq. (40b); final number of integration intervals = 2^{ic+1}

7. is, the number of iterations required to calculate the integral in Eq. (40c); final number of integration intervals = 2^{is+1}

8. fix, the value of the integral G_x in Eq. (40a)

9. fic, the value of the integral G_c in Eq. (40b)

10. fie, fix + fic, the even integral part G_e

11. fio, the value of the integral G_o in Eq. (40c), the odd integral part

12. fit, fie + fio, the total green's function G_0

The last line gives the CPU time in seconds needed to calculate fie, fio, and fit.

The results of Table 3 confirm the expected symmetry of all five integrals about $y = 0$, the symmetry of fix, fic, and fie about $x = 0$, and the antisymmetry of fio about $x = 0$.

3.6 Computer Time Requirements

Computer time depends on various factors, of which the x,y, and z values of the field point, the error criterion erc, the type of integral, and the integration rule are most important. Tables 4a, b, and c respectively show, for the trapezoidal rule, the effect of different values of x,z, and erc on average CPU time per field point (in seconds) using the Hewlett Packard 9000, Model 550 minicomputer. Tables 5a to c show corresponding times using Simpson's rule. In all cases, times are shown for fie, fio, and fit. Consider first the trapezoidal rule case shown in Table 4. Table 4a shows that for fixed values of z and erc, computer time increases as values of x_M increase from 1 to 50, 25-fold in the case of fie and 3-fold in the case of fio. Table 4b shows that for fixed values of x_M and erc, computer time increases with values of z decreasing from 1.0 to 0.001, 3-fold in the case of fie and over 100-fold in the case of fio. The large increase in the latter case is directly related to the need to use higher values of u_M with decreasing z, as shown in Table 1. Finally, for fixed values of x_M and z, Table 4c shows the expected trend of computer time increasing as the allowable error erc is decreased from 0.01 to 0.0001, the increase being 10-fold for fie and 3-fold for fio.

Comparison of the time requirements for the Simpson's rule in Table 5 with corresponding times for the trapezoidal rule in Table 4 shows that the use of the higher order Simpson's rule typically results in a 3- to 4-fold decrease in the case of fie and (somewhat surprisingly) a 50 to 100% increase in the case of fio. This may be due to the fact that the relatively smooth integrands of fie benefit from the parabolic fit through the points used in Simpson's rule, while the oscillatory integrand of fio seems to be better approximated by the straight line fit of the trapezoidal rule.

4. CALCULATED RESULTS

In this chapter we will present sample calculated results obtained by using Program KELGREEN. First, our calculated results are recast in the form of near field (G_n) and far field (G_f) components, and the values of G_n are then compared with exact values contained in [4]. Secondly, three-dimensional and contour plots of G_x, G_c, G_e, G_o, and G_0, defined in Eq. (40), are given to show the overall behavior of these integrals. Finally, line plots of these integrals are given to show the finer details of their individual and relative behavior.

4.1 Numerical Checks

Since Newman [4] decomposes G_0 into near and far field components G_n and G_f, we must recast our formulation, which is in terms of G_e and G_o, to Newman's form. Actually, this is simply done by noting that

$$G_f = 2\, G_o \qquad x \geq 0 \tag{43}$$

and

$$G_0 = G_n + G_f = G_n + 2\, G_o = G_e + G_o \tag{44}$$

to obtain G_n in terms of G_e and G_o

$$G_n = G_e - G_o \tag{45}$$

Newman gives accurately calculated values of G_n for the three sets of field points (R, 0, 0,), (0, R, 0), and (0, 0, R) where $R = 1,4,10$. The last two sets are most convenient for us to calculate and we shall discuss these first. For both of these cases, $x = 0$, where $G_o = 0$, and Eq. (45) then shows

$$G_n \equiv G_e \qquad \text{at } x = 0 \tag{46}$$

Accordingly, Tables 6a and b respectively show comparisons between our G_e and Newman's G_n for these two cases of $x = 0$. Table 6 shows that there usually is agreement to four decimal places, as may expected from the erc $= 0.0001$ used to calculated G_e.

The set (R, 0, 0) is more troublesome to calculate for both G_e and G_o. These troubles have already been pointed out in the preceding chapter. In the case of G_o, $z = 0$ implies that the exponential convergence factor $\exp(-s^2 z) = 1$, and a theoretical infinite upper limit of integration umx may be required. In the case of G_e, $y = z = 0$ lead to $\rho = 0$ and $x/\rho \to \infty$, again an infinite upper limit of integration for G_x, given in Eq. (40a). For both of these reasons, z must be given a value >0 in our approach. Table 7 lists our calculated values of G_n for $R = 1,4,10$ and $z = 0.001$, 0.01, and 0.1 using erc $= 0.001$. For comparison purposes, the table also lists Newman's values which correspond to $z = 0$. As may be expected, the agreement with Newman's values increases with decreasing values of z. Thus, there is essentially agreement to three decimal places for $z = 0.001$, two to three places in the case of $z = 0.01$, and one to two places for $z = 0.1$. A simpler way of conducting this check is given in [9] by making use of specialized analyses for G_o and G_x for $\rho = 0$.

4.2 Overall Three-Dimensional and Contour Plots

Figures 3a, b, c, d, and e respectively show three-dimensional plots of G_x, G_c, G_e, G_o, and G_0 for the case of $z = 0.1$ over a 101×41 rectangular grid with $0 \le x \le 50$, and $0 \le y \le 20$. To illustrate the effect of z, Figs. 4a and b respectively show G_e for $z = 0.01$ and $z = 1.0$. Figures 5a-e and 6a-b show the corresponding contour plots of the cases given in Figures 3a-e and 4a-b.

Figure 3a shows that the largest waves of G_x are confined in a triangular region which does not extend to the x axis. Figure 3b shows that the wave pattern for G_c is relatively simple, consisting of waves whose amplitudes decrease with increasing distance from the x axis. Figure 3c shows that the wave pattern of the resultant even integral G_e is confined to a triangular sector whose sides are the x axis and a cusp line at approximately 20 degrees, i.e., the familiar Kelvin wake. Figures 3c, d, and e show that the even integral G_e, the odd integral G_o, and the total function G_0 all have similar wave patterns. This is not surprising since far upstream the (symmetric about $x = 0$) G_e and the (antisymmetric about $x = 0$) G_o must exactly cancel to give $G_0 = 0$. Thus, for the positive values of x shown in Figure 3, the values of G_e and G_o tend to be equal for increasing x and G_0 is then simply 2 G_e or 2 G_o. This upstream cancellation and downstream reinforcement is shown more clearly in the line plots given in the following section. The above described behavior is shown in a somewhat different and clearer form by the contour plots given in Figs. 5 a-e. In particular, Figs. 5c-e show the overall striking similarity between G_e, G_o, and G_0 for large values of x. However, Figs. 5c and d do show that near $x = 0$, there are substantial differences between G_e and G_o, with G_e exhibiting a vertical bubble outside of the Kelvin sector.

In the case of G_e, Figs. 4a, 3c, and 4b respectively show the well known disappearance of the short waves near the cusp line as z increases from 0.01 to 0.1 and 1.0. Another way of stating this is that the transverse waves tend to gain in prominence as z increases. Similarly, the contour plots given in Figs. 6a, 5c, and 6b show the progressive disappearance of the clutter corresponding to the short waves as z increases.

4.3 Detailed Line Plots

Figures 7a, b, c, and d respectively show line plots of the component integrals G_x, G_c, and G_o at $y = 0,2,4$, and 6 for $z = 0.1$ and $0 \leq x \leq 20$. To obtain a view of the behavior of the integrals over a wider range of x, including upstream values, Figs. 8a, b respectively show plots of G_0 at $y = 0,10$ for $z = 0.1$ and $-100 \leq x \leq 100$. Making use of the previously mentioned symmetry properties of G_e and G_o about $x = 0$, G_0 for negative values of x is simply computed from corresponding results for positive values of x, as follows

$$G_0(-x) = G_e(x) - G_o(x) \tag{47}$$

Figure 7 shows that the relative behavior between the component integrals varies with the location y. Figure 7a shows that on the x axis, $y = 0$, the even integral component G_c resembles the odd integral G_o, while the component G_x serves as a correction factor indicating the differences between G_e and G_o. At off axis locations, $y > 0$, Figs. 7b-e show that the reverse is true, i.e., now G_x resembles G_o, while G_c tends to serve as the correcting factor. This behavior may be deduced to some extent from the three-dimensional and contour plots of the preceding section. Results for $z = 0.01$ and $z = 1.0$ which are not shown exhibit similar relative behavior between the component integrals.

Figures 8a and b show the expected trend that $G_0 \rightarrow 0$ far upstream for both $y = 0$ and 10. This is another verification of the accuracy of our approach, i.e., the separate calculations of G_e and G_o do indeed combine to give the required annullment far upstream. The upstream extent of the local disturbance is relatively small and decays rapidly near the origin.

5. SUMMARY

Computer code KELGREEN has been developed to calculate the complete wave resistance Green's function G_0 for the case of a nonoscillating source translating below the free surface. The numerical implementation is based on the unique work of Bessho, who succeeds in representing G_0 as a single integral in the complex plane. We have recast this integral as three real single integrals G_x, G_c, and G_s, where $G_x + G_c$ correspond to the double or even integral G_e and the third integral to the single or odd integral G_o in the usual representation of G_0. By simple rearrangement, we can also express our results in terms of the more physical near and far field components, G_n and G_f. Computer time requirements depend on a number of factors, principally the integration rule used, the submergence of the source z, the error criterion erc, and the distance of the field point from the source ρ. For most cases, CPU time for a calculation of G_0 at one field point is typically 0.5 to 2 seconds on the Hewlett Packard 9000, Model 550 minicomputer. Compared to the trapezoidal rule, use of the higher order Simpson's rule typically reduces CPU time 3- to 4-fold, in the case of G_e, but increases CPU time 1.5- to 2-fold in the case of G_o. It seems that the parabolic fit used in Simpson's rule is not a good approximation for the highly oscillatory integrand of G_o.

A number of checks have been performed on the accuracy of our numerical analysis and computer code development. For field points located on each of the three coordinate axes, our calculated values for the near field component agree well with exact results. Also, the calculated results show the required mutual annulment of our integrals in the far upstream region. A number of three-dimensional and contour plots are given to show the overall behavior of the various integral components. These plots show the general resemblance of G_e to G_o in the far field, and the differences between G_e and G_o in the near field. Line plots show the fact that near the x axis G_c resembles G_o while away from the x axis G_x resembles G_o.

6. ACKNOWLEDGMENT

This work was conducted as part of a research program in free surface and marine hydrodynamics supported by the Naval Research Laboratory and Code 12 of the Office of Naval Research. The second author performed this work under the sponsorship of the U.S. Navy-ASEE Summer Faculty Research Program.

7. REFERENCES

1. Michell, J.H., "The Wave Resistance of a Ship," *Philosophical Magazine*, Vol. 45, No. 272, pp. 106-123, January 1898.

2. Eggers, K.W.H., Sharma, S.D., and Ward, L.W., "An Assessment of Some Experimental Methods for Determining the Wavemaking Characteristics of a Ship Form," *Transactions of the Society of Naval Architects and Marine Engineers*, Vol. 75, pp. 112-157, November 1967.

3. Noblesse, F., "Alternative integral representations for the Green function of the theory of ship wave resistance," *Journal of Engineering Mathematics*, Vol. 15, No. 4, pp. 241-265, October 1981.

4. Newman, J.N., "Evaluation of the Wave-Resistance Green Function: Part I - The Double Integral," *Journal of Ship Research*, Vol. 31, No. 2, pp. 79-90, June 1987.

5. Abramowitz, M. and Stegun, I.A., *Handbook of Mathematical Functions with Formulas, Graphs, and Mathematical Tables*, U.S. Government Printing Office, Washington, D.C., June 1964.

6. Bessho, M., "On the Fundamental Function in the Theory of the Wave-Making Resistance of Ships," *Memoirs of the Defense Academy, Japan*, Vol. 4, No. 2, pp. 99-119, 1964.

7. Ursell, F., "Mathematical Note on the Fundamental Solution (Kelvin Source) in Ship Hydrodynamics," *IMA Journal of Applied Mathematics*, Vol. 32, pp. 335-351, 1984.

8. Wehausen, J.V. and Laitone, E.V., "Surface Waves," *Encyclopedia of Physics*, Vol. 9, Springer-Verlag, Berlin, pp. 446-778, 1960.

9. Wang, H.T. and Rogers, J.C.W., "Numerical Evaluation of the Complete Wave-Resistance Green's Function Using Bessho's Approach," *Fifth International Conference on Numerical Ship Hydrodynamics*, September 1989.

10. Euvrard, D., "Les mille et une facéties de la fonction de Green du problème de la resistance de vagues," Ecole Nationale Supérieure de Techniques Avancées Report 144, June 1983.

8. APPENDIX — BEHAVIOR OF G_0 FOR SMALL ρ, LARGE $|x|$

In view of the numerical difficulties encountered by G_o and G_x for $z \to 0$ and $\rho \to 0$, respectively, it is of interest to investigate the bavhavior of G_o near the x-axis, $\rho \to 0$. We derive here an expression for the first order far field behavior of G_o in the neighborhood of $\rho = 0$. Since Eq. (45) shows that G_e differs from G_o by the well behaved near field component G_n, then any type of singular behavior experienced by G_o must also be true for G_e.

We start with the expression for G_o given in Eq. (37) and decompose the integration interval into two parts

$$G_o = 4\left[\int_0^{1/2} + \int_{1/2}^{\infty}\right] \sin(x\sqrt{t^2+1})\cos(yt\sqrt{t^2+1})\, e^{-(t^2+1)z}\, dt$$

$$= I_1 + I_2 \tag{A1}$$

Basically, the integral I_1 will furnish the asymptotic behavior for large $|x|$ while I_2 will furnish the behavior around $\rho = 0$. In the course of the derivation, it will be seen that the intermediate limit, taken to be 1/2, is somewhat arbitary as long it is of O(1).

To obtain the behavior of I_1, let us make the change of variables

$$\sqrt{t^2+1} - 1 = u^2 \to t = u\sqrt{2+u^2} \tag{A2a}$$

$$dt = \frac{2(1+u^2)}{\sqrt{2+u^2}}\, du \tag{A2b}$$

Use of Eq. (A2a) gives the following expansion of the sine term in terms of u

$$\sin(x\sqrt{t^2+1}) = \sin x \cos(xu^2) + \cos x \sin(xu^2) \tag{A3}$$

Noting that $1/\sqrt{2+u^2}$ can be expanded in powers of u and (for $\rho \to 0$) the exponential and cosine factors in Eq. (A1) can be expanded in powers of z and y, respectively, it can be seen that I_1 consists of summing the following two types of series

$$I_1 \to \sum_n \int_0^a \cos(xu^2)\, u^n\, du + \sum_n \int_o^a \sin(xu^2)\, u^n\, du \tag{A4}$$

where $a = (\sqrt{5/4} - 1)^{1/2}$ for the intermediate limit of 1/2 chosen in Eq. (A2). For $n = 0$ we have

$$\int_o^a \sin(xu^2)du = \left[\int_0^{\infty} - \int_a^{\infty}\right] \sin(xu^2)du$$

$$= \frac{1}{2}\sqrt{\frac{\pi}{2|x|}}\,\mathrm{sgn}(x) - \frac{\cos(xa^2)}{2xa} - \frac{\sin(xa^2)}{4x^2a^3} + \frac{3}{4x^2}\int_a^{\infty} \frac{\sin(xu^2)}{u^4}\, du$$

$$= \frac{1}{2}\sqrt{\frac{\pi}{2|x|}}\,\mathrm{sgn}(x) + \text{terms of } O(\frac{1}{x}) \tag{A5}$$

Similarly, for the cosine integral in Eq. (A2) we obtain

$$\int_0^a \cos(xu^2)\,du = \left[\int_0^\infty - \int_a^\infty\right] \cos(xu^2)\,du$$

$$= \frac{1}{2}\sqrt{\frac{\pi}{2|x|}} + O(\frac{1}{x}) \tag{A6}$$

For $n = 1$, we obtain

$$\int_0^a u\cos(xu^2)\,du = \frac{1}{2x}\sin(xa^2) = O(\frac{1}{x}) \tag{A7a}$$

$$\int_0^a u\sin(xu^2)du = \frac{1}{2x}[1 - \cos(xa^2)] = O(\frac{1}{x}) \tag{A7b}$$

Results for $n \geq 2$ may be expressed in terms of corresponding values at lower values of n, as follows

$$\int_0^a u^n [\cos(xa^2)\,du, \sin(xu^2)]\,du = \frac{d}{dx}\int_o^a u^{n-2}[\sin(xu^2), -\cos(xu^2)]\,du \tag{A8}$$

which are $O\left[\frac{1}{x^{3/2}}\right]$ or higher. Thus, retaining only the lowest order term as $|x| \to \infty$, the asymptotic expression for I_1 is given by summing Eqs. (A5) and (A6) and multiplying by 4

$$I_1 \to 2\sqrt{\frac{\pi}{|x|}}\,[\sin x + \mathrm{sgn}(x)\cos x]\,e^{-z} \tag{A9}$$

For evaluation of the integral I_2, we consider G_o in terms of the variable s, defined in Eq. (39), to obtain

$$I_2 = 4\int_{\sqrt{5/4}}^\infty \sin(xs)\cos(ys\sqrt{s^2-1})\,e^{-s^2z}\,\frac{s}{\sqrt{s^2-1}}\,ds \tag{A10}$$

Following Euvrard [9], the last factor is decomposed as follows

$$\frac{s}{\sqrt{s^2-1}} = \frac{1}{(s+\sqrt{s^2-1})(\sqrt{s^2-1})} + 1 \tag{A11}$$

to split I_2 into two integrals $I_3 + I_4$, which respectively contain the first and second factors. By integraion by parts, we see that $I_3 = O(\frac{1}{|x|})$ as $|x| \to \infty$.

To find the behavior of I_4 we rewrite the cosine factor in Eq. (A10) according to the substitution

$$s\sqrt{s^2-1} = s^2 - \frac{s}{s+\sqrt{s^2-1}} = s^2 - \frac{1}{2} - \frac{1}{2(s+\sqrt{s^2-1})^2} \tag{A12}$$

and further expand the resulting trigonometric terms involving $[y/2(s + \sqrt{s^2 - 1})^2]$ in a power series (noting that y is assumed small in our analysis). After conisderable algebra, we find that the only contribution which is not of O $(\frac{1}{|x|})$ or higher is of the form

$$I_5 = 4 \int_0^\infty \sin(xs) \cos[y(s^2 - \frac{1}{2})]\, e^{-s^2 z}\, ds$$

$$= 2 \int_0^\infty \sin[xs + y(s^2 - \frac{1}{2})]\, e^{-s^2 z} ds + 2 \int_0^\infty \sin[xs - y(s^2 - \frac{1}{2})]\, e^{-s^2 z}\, ds \quad \text{(A13)}$$

where changing the lower limit of $\sqrt{5/4}$ in Eq. (A10) to 0 makes only a contribution of O $(\frac{1}{|x|})$. Noting that the above integral is odd in x and even in y, there is no loss in generality in restricting our analysis to $x > 0$, $y > 0$. The last equality in Eq. (A13) suggests the following alternate decomposition of I_5 in terms of complex integrals

$$I_5 = 2 \text{ Im } (I_7) + 2 \text{ Im } (I_8) \quad \text{(A14)}$$

$$I_7 = \int_0^\infty e^{i[xs + y(s^2 - \frac{1}{2})] - z s^2} ds \quad \text{(A15a)}$$

$$I_8 = \int_0^\infty e^{i[xs - y(s^2 - \frac{1}{2})] - z s^2} ds \quad \text{(A15b)}$$

The evaluation of I_7 proceeds by rewriting it in the following form

$$I_7 = \int_0^\infty e^{(iy - z)(s + \frac{ix}{2(iy - z)})^2} ds\, e^{\frac{x^2}{4(iy - z)}}\, e^{-iy/2}$$

$$= \int_u^\infty e^{(iy - z)\zeta^2} d\zeta\, e^{-u^2 (iy - z)}\, e^{-iy/2} \quad \text{(A16)}$$

where $\zeta = s + ix/[2(iy - z)]$ and $u = x/2(y + iz)$. The first integration by parts gives a term of O$(\frac{1}{x})$ while each successive integration gives terms whose order increases by $1/x^2$. Thus, compared to I_1, I_7 may be neglected.

The evaluation of I_8 starts by rewriting it in the following form, similar to the procedure used for I_7

$$I_8 = \int_0^\infty e^{(iy + z)(s - \frac{ix}{2(iy + z)^2})^2} ds\, e^{\frac{-x^2}{4(iy - z)}}\, e^{iy/2}$$

$$= \int_u^\infty e^{-(iy + z)\zeta^2} d\zeta\, e^{u^2 (iy + z)}\, e^{iy/2} \quad \text{(A17)}$$

By rewriting the integration interval as follows

$$\int_u^\infty = \int_{-\infty}^\infty - \int_{-\infty}^u \quad \text{(A18)}$$

we note that the first integral on the right hand side can be evaluated in closed form

$$I_8 = \frac{\sqrt{\pi}}{\sqrt{z+iy}}\, e^{-\frac{x^2}{4(iy+z)}}\, e^{iy/2} - e^{u^2\,(iy+z)}\, e^{iy/2} \int_{-\infty}^{u} e^{-(iy+z)\,\zeta^2}\, d\zeta \qquad \text{(A19)}$$

As in the case of I_7 integration by parts of the integral on the right hand side yields terms of $O(\frac{1}{|x|})$ or higher.

Discarding terms of the order $1/|x|$ as $|x| \to \infty$, we get as a first order approximation for the asymptotic behavior of G_o the sum of I_1, given in Eq. (A9), and twice the imaginary part of the first term of I_8, given in Eq. (A19)

$$G_o \to \mathrm{sgn}(x)\, 2\sqrt{\frac{\pi}{\rho}}\, e^{-\frac{x^2 z}{4(y^2+z^2)}} \sin\left[\frac{x^2 y}{4(y^2+z^2)} + \frac{y}{2} - \frac{\alpha}{2}\right]$$

$$+ 2\sqrt{\frac{\pi}{|x|}}\, (\sin x + \mathrm{sgn}(x) \cos x)\, e^{-z} \qquad \text{(A20)}$$

This equation confirms the two specialized limiting trends observed by Euvrard [10] that (1) the behavior is singular for $z = 0$, $y \to 0$ and (2) the behavior is regular for $y = az$ ($a \neq \pm\infty$), $z \to 0$. Our generalized equation further shows that the limit behavior will be regular along any curve $y = z^n$, $n > \frac{1}{2}$, and singular for $n \leq \frac{1}{2}$. The above two trends noted by Euvrard respectively correspond to $n = 0$ and $n = 1$.

Table 1 — Required Values of the Upper Limit of Integration u_M in G_o for Various Error Values ϵ and Source Submergences z

ϵ	$z = 1.0$	$z = 0.3$	$z = 0.1$	$z = 0.03$	$z = 0.01$	$z = 0.003$
0.01	4.2	17.	55.	200.	660.	2400.
0.001	6.2	24.	77.	280.	880.	3100.
0.0001	8.4	31.	99.	350.	1100.	3900.

Table 2- Sample Input File

```
osample
0.10 07 03 -2. 2. -1. 1. 75. 20. 0.001 30 2 1
```

Table 3- Sample Formatted Output File

z,erc,umx,xpmx= .100000 .001000 75.00 20.00

x	y	x/rh	alfa	ix	ic	is	fix	fic	fie	fio	fit
-2.00	-1.00	-2.0	-84.3	3	2	8	3.1643	-.1176	3.0467	-2.4235	.6232
-2.00	.00	-20.0	.0	6	3	8	1.4748	-.0148	1.4600	-.8166	.6434
-2.00	1.00	-2.0	84.3	3	2	8	3.1643	-.1176	3.0467	-2.4235	.6232
.00	-1.00	.0	-84.3	1	2	1	.0000	1.5430	1.5430	.0000	1.5430
.00	.00	.0	.0	1	2	1	.0000	3.7437	3.7437	.0000	3.7437
.00	1.00	.0	84.3	1	2	1	.0000	1.5430	1.5430	.0000	1.5430
2.00	-1.00	2.0	-84.3	3	2	8	3.1643	-.1176	3.0467	2.4235	5.4702
2.00	.00	20.0	.0	6	3	8	1.4748	-.0148	1.4600	.8166	2.2765
2.00	1.00	2.0	84.3	3	2	8	3.1643	-.1176	3.0467	2.4235	5.4702
4.00	-1.00	4.0	-84.3	5	3	8	-2.5340	-1.0075	-3.5415	-3.9286	-7.4701
4.00	.00	40.0	.0	6	4	8	.6205	-2.5201	-1.8996	-2.2914	-4.1911
4.00	1.00	4.0	84.3	5	3	8	-2.5340	-1.0075	-3.5415	-3.9286	-7.4701
6.00	-1.00	6.0	-84.3	6	2	8	1.6743	.5970	2.2713	1.9907	4.2619
6.00	.00	60.0	.0	6	5	8	.3880	.8668	1.2548	.9724	2.2272
6.00	1.00	6.0	84.3	6	2	8	1.6743	.5970	2.2713	1.9907	4.2619
8.00	-1.00	8.0	-84.3	7	2	8	1.0809	.2354	1.3163	1.0961	2.4125
8.00	.00	80.0	.0	6	5	8	.2811	.8567	1.1378	.9170	2.0548
8.00	1.00	8.0	84.3	7	2	8	1.0809	.2354	1.3163	1.0961	2.4125
10.00	-1.00	10.0	-84.3	7	3	8	-.6567	-.7715	-1.4282	-1.6084	-3.0366
10.00	.00	100.0	.0	6	6	8	.2200	-1.4543	-1.2343	-1.4152	-2.6496
10.00	1.00	10.0	84.3	7	3	8	-.6567	-.7715	-1.4282	-1.6084	-3.0366

time even,odd,tot= 3.00 14.00 17.00

Table 4 — Variation of Average CPU Time in Seconds for Different Values of x_M, z, and erc, Trapezoidal Rule

(a) $0 \le x \le x_M$, $z = 0.1$, $erc = 0.001$, x_M variable			
x_M	fie	fio	fit
1.0	0.05	0.47	0.52
5.0	0.27	0.62	0.89
20.0	0.65	0.98	1.64
50.0	1.24	1.42	2.66
(b) $0 \le x \le 20$, $erc = 0.001$, z variable			
z	fie	fio	fit
0.01	1.78	10.70	12.48
0.1	0.65	0.98	1.64
0.3	0.52	0.29	0.82
1.0	0.57	0.10	0.66
(c) $0 \le x \le 20$, $z = 0.1$, erc variable			
erc	fie	fio	fit
0.01	0.21	0.56	0.77
0.001	0.65	0.98	1.64
0.0001	2.05	1.46	3.50

Table 5 — Variation of Average CPU Time in Seconds for Different Values of x_M, z, and erc, Simpson's Rule

(a) $0 \le x \le x_M$, $z = 0.1$, $erc = 0.001$, x_M variable			
x_M	fie	fio	fit
1.0	0.02	0.66	0.68
5.0	0.06	1.06	1.12
20.0	0.19	1.55	1.74
50.0	0.49	2.67	3.16
(b) $0 \le x \le 20$, $erc = 0.001$, z variable			
z	fie	fio	fit
0.01	0.46	18.05	18.51
0.1	0.19	1.55	1.74
0.3	0.16	0.51	0.67
1.0	0.15	0.14	0.29
(c) $0 \le x \le 20$, $z = 0.1$, erc variable			
erc	fie	fio	fit
0.01	0.10	0.86	0.96
0.001	0.19	1.55	1.74
0.001	0.33	2.49	2.82

Table 6 — Comparison of Calculated Values of G_e with Newman's Benchmark Values of G_n, $erc = 0.0001$, $x = 0$

R	(a) (0, R, 0)		(b) (0,0,R)	
	G_e	G_n	G_e	G_n
1	1.4495975	1.4495569	2.1523585	2.1523180
4	0.6399984	0.6399881	0.6026911	0.6026808
10	0.2314356	0.2314102	0.2121567	0.2121503

Table 7 — Comparison of Calculated Values of G_n with Newman's Benchmark Values, (R,0,0), $erc = 0.001$

	Newman ($z \equiv 0$)	$z = 0.001$	$z = 0.01$	$z = 0.1$
$R = 1$	0.9223	0.9226	0.9268	0.9642
$R = 4$	0.3895	0.3899	0.3904	0.3923
$R = 10$	0.1805	0.1820	0.1812	0.1812

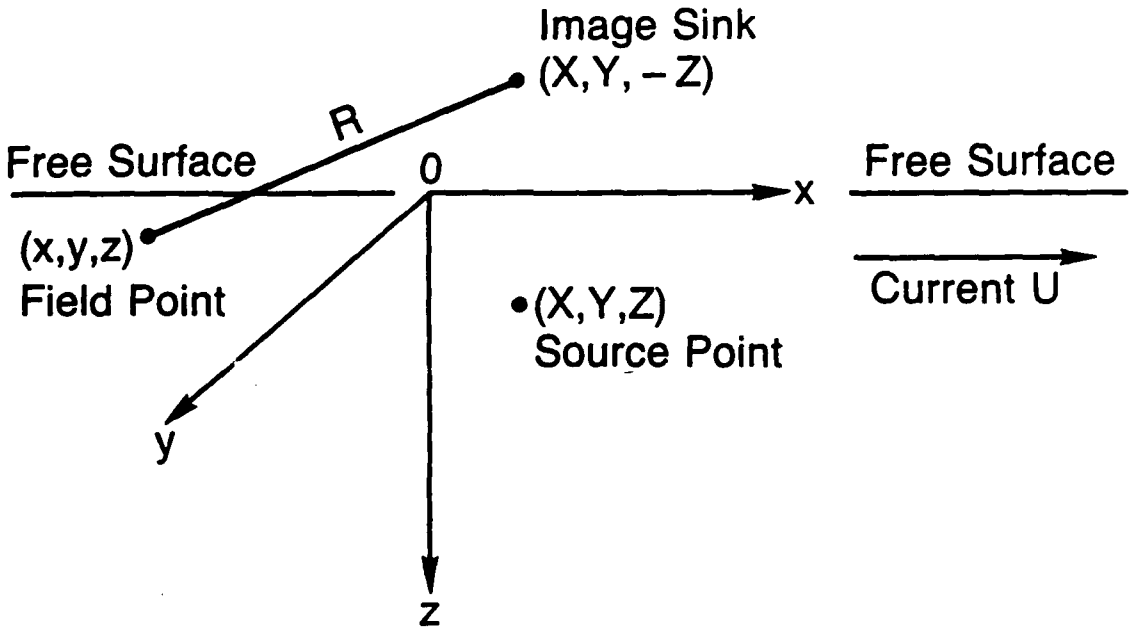

Fig. 1 — Definition of coordinate system

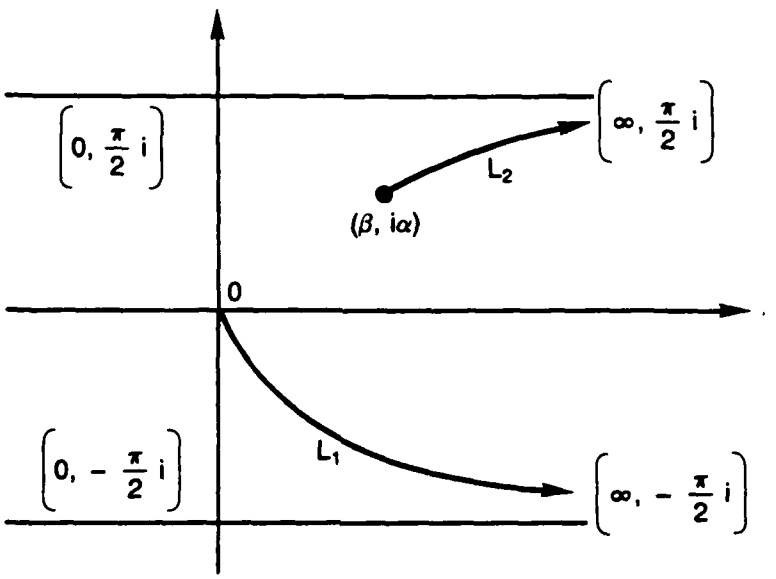

Fig. 2 — Bessho's integration path in the complex ν-plane

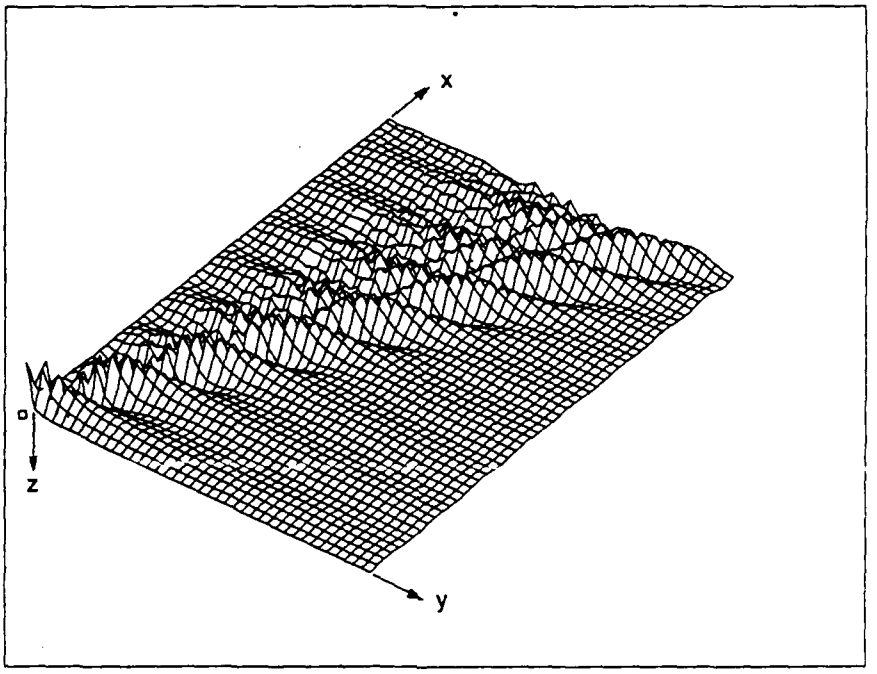

Fig. 3(a) — Integral G_x

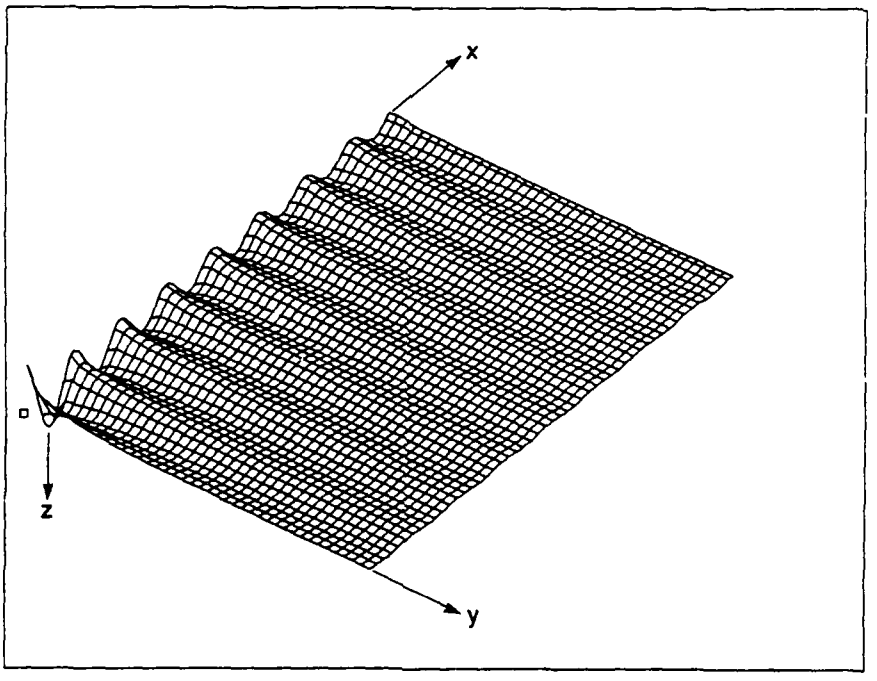

Fig. 3(b) — Integral G_c

Fig. 3 — Three-dimensional plots of component integrals, $z = 0.1$

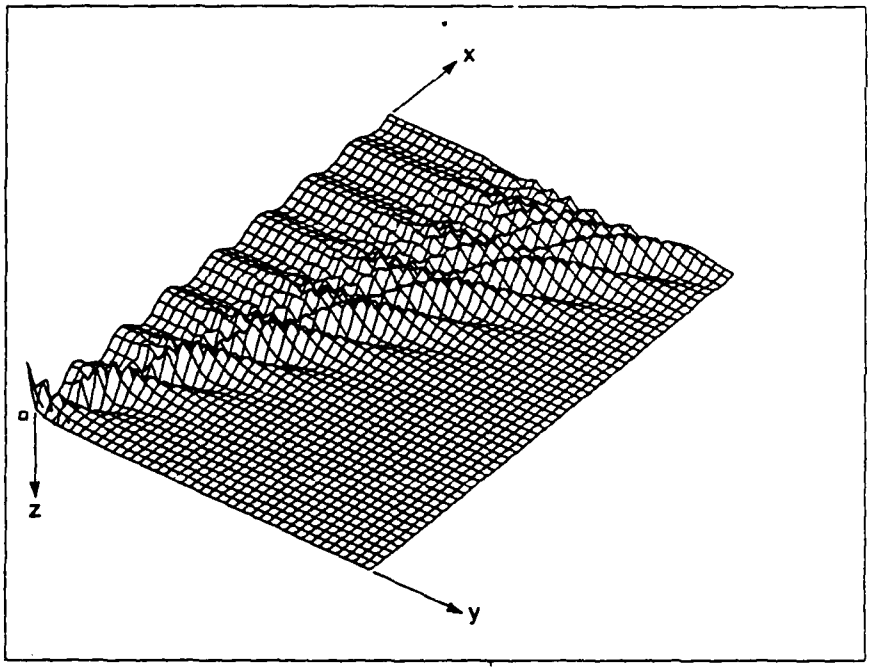

Fig. 3(c) — Integral G_e

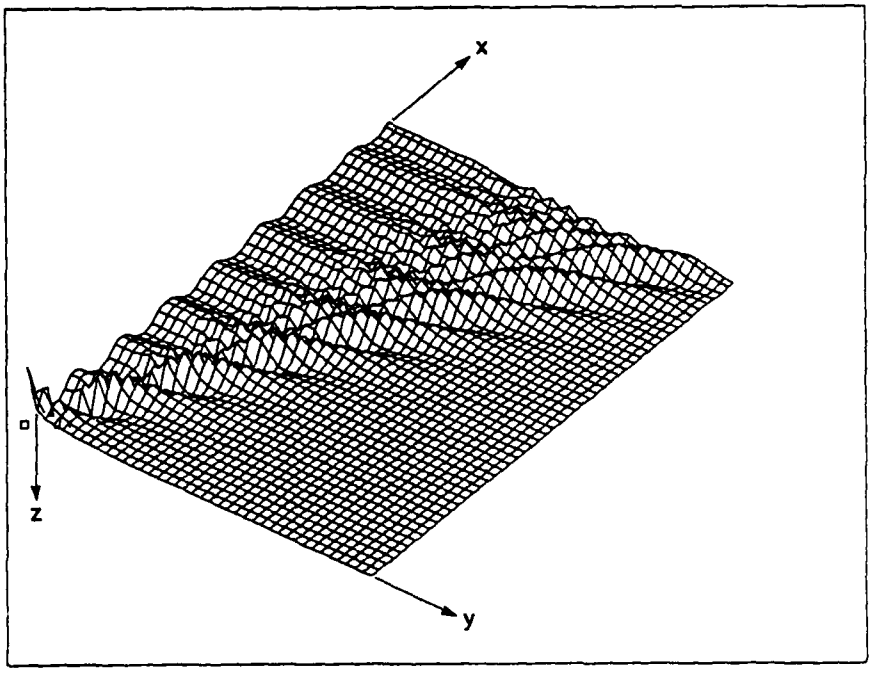

Fig. 3(d) — Integral G_o

Fig. 3 — (Continued) Three-dimensional plots of component integrals, $z = 0.1$

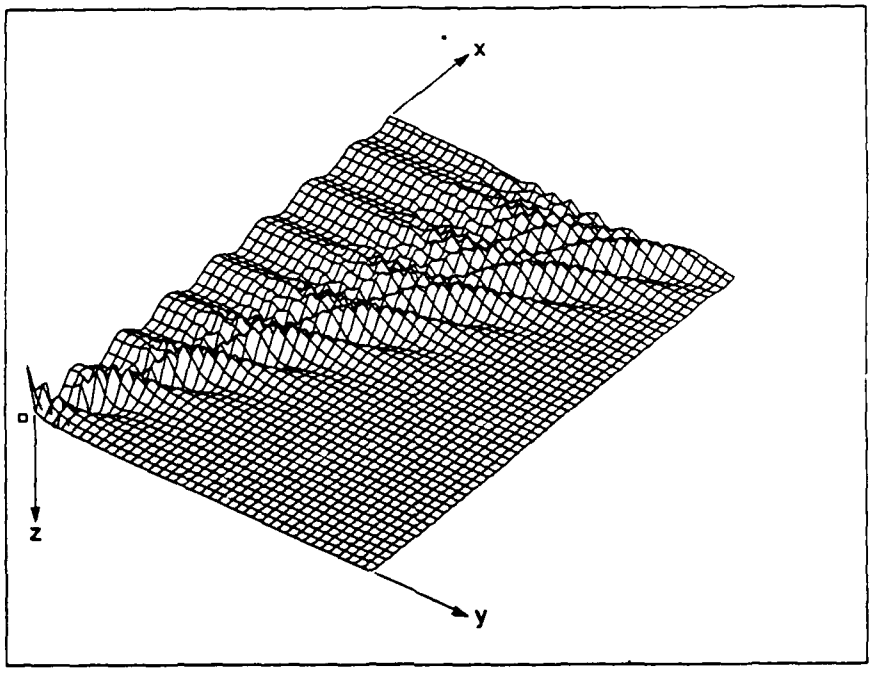

Fig. 3(e) — Integral G_0

Fig. 3 — (Continued) Three-dimensional plots of component integrals, $z = 0.1$

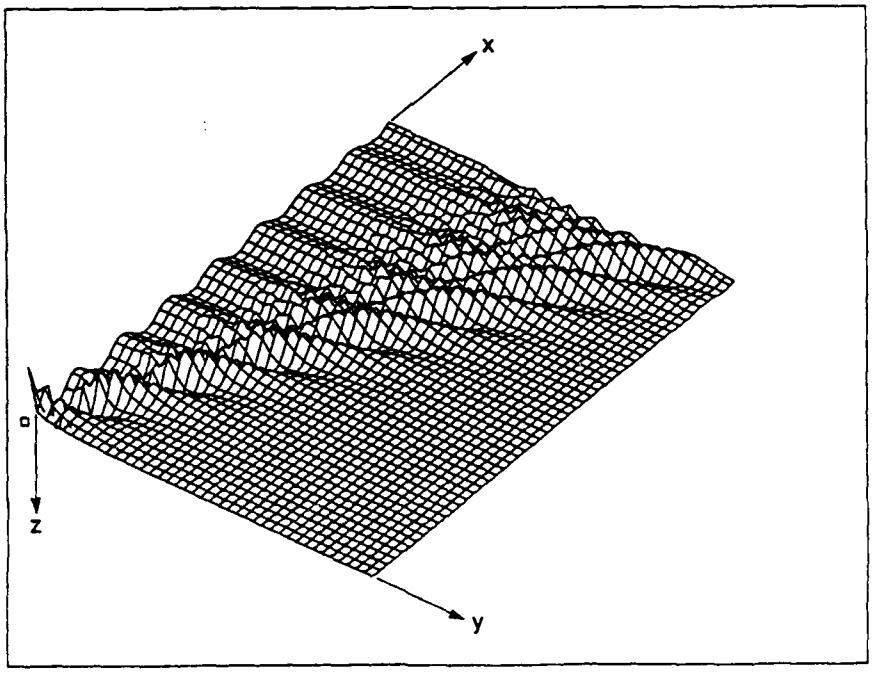

Fig. 4(a) — $z = 0.01$

Fig. 4 — Three-dimensional plots of G_e

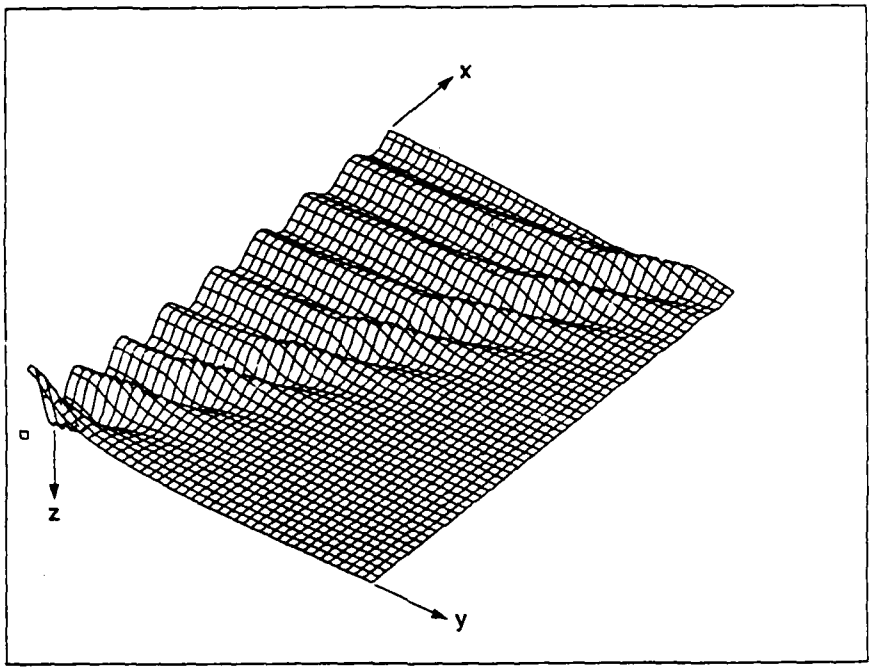

Fig. 4(b) — $z = 1.0$

Fig. 4 — (Continued) Three-dimensional plots of G_e

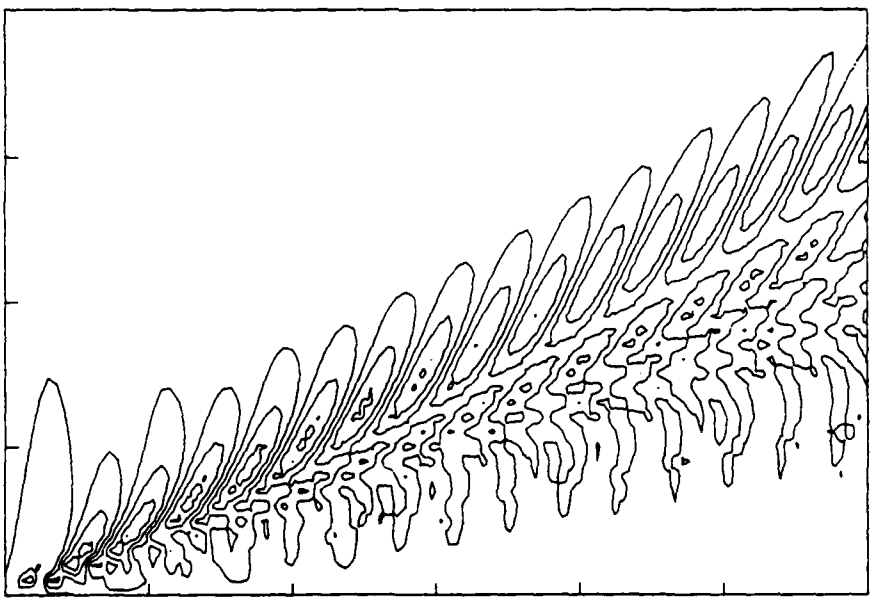

Fig. 5(a) — Integral G_x

Fig. 5 — Contour plots of component integrals, $z = 0.1$

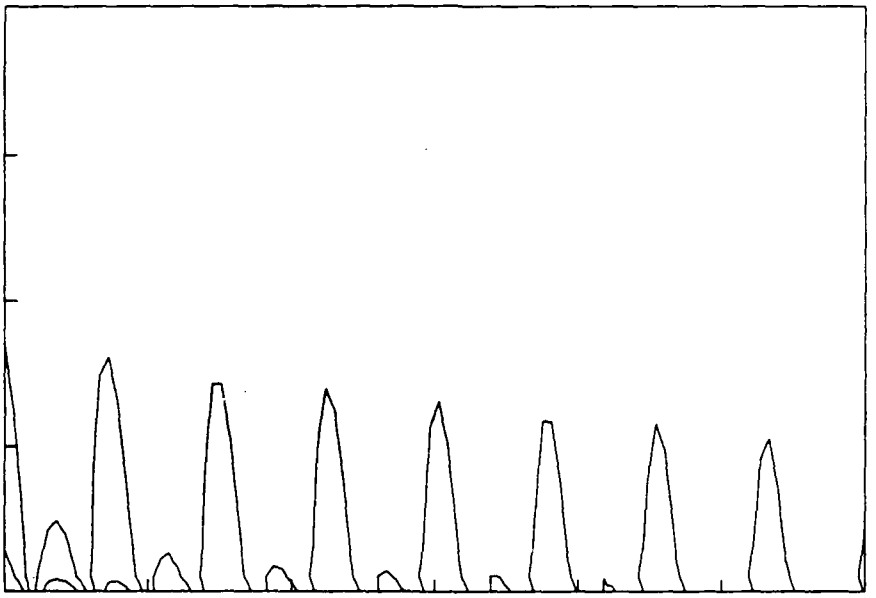

Fig. 5(b) — Integral G_c

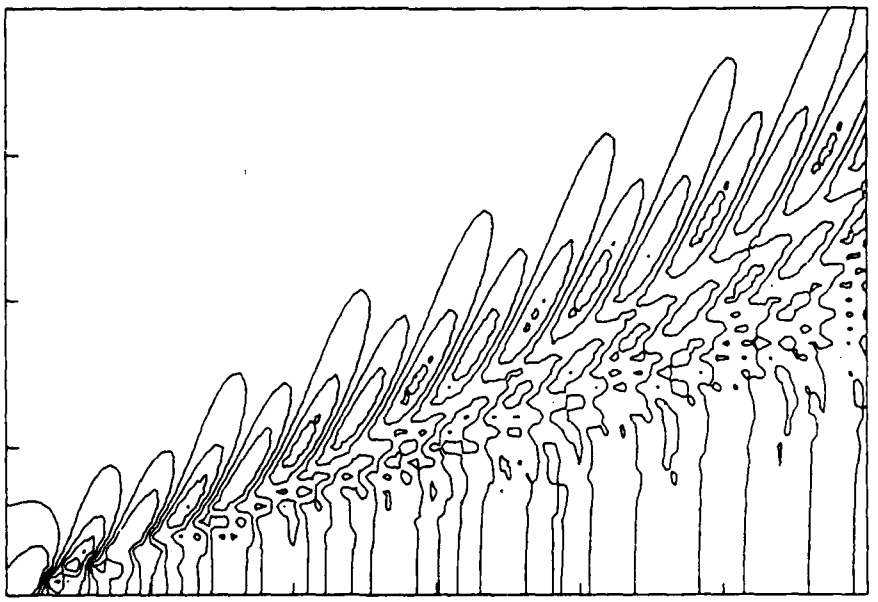

Fig. 5(c) — Integral G_e

Fig. 5 — (Continued) Contour plots of component integrals, $z = 0.1$

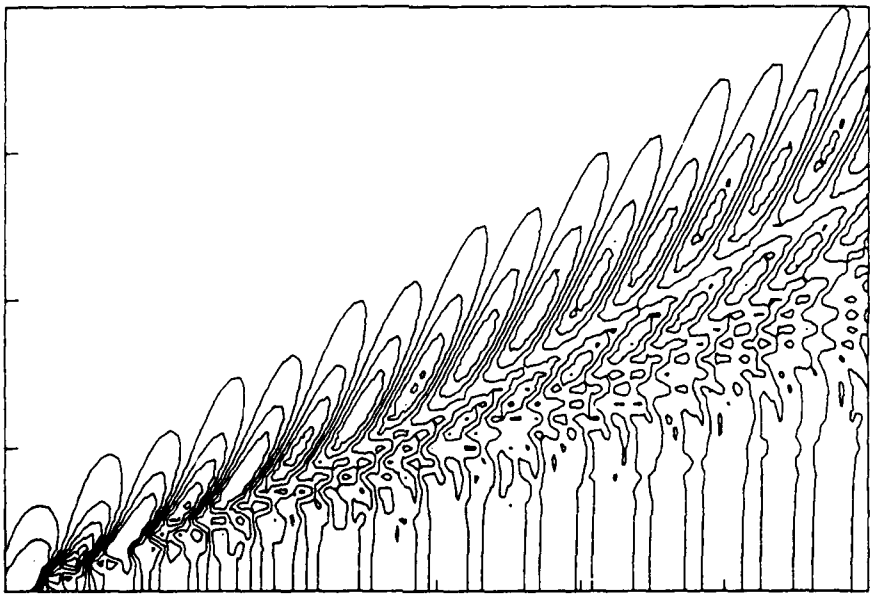

Fig. 5(d) — Integral G_o

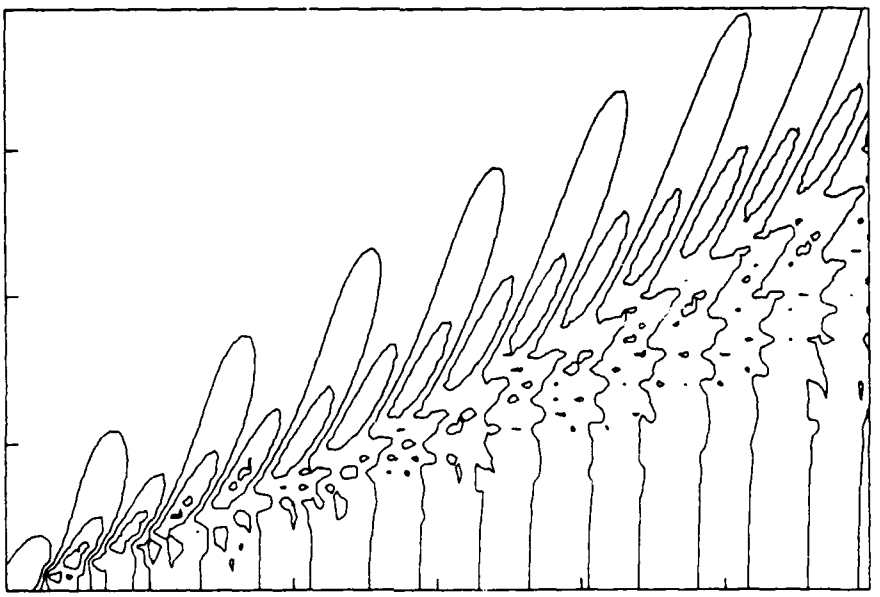

Fig. 5(e) — Integral G_0

Fig. 5 — (Continued) Contour plots of component integrals, $z = 0.1$

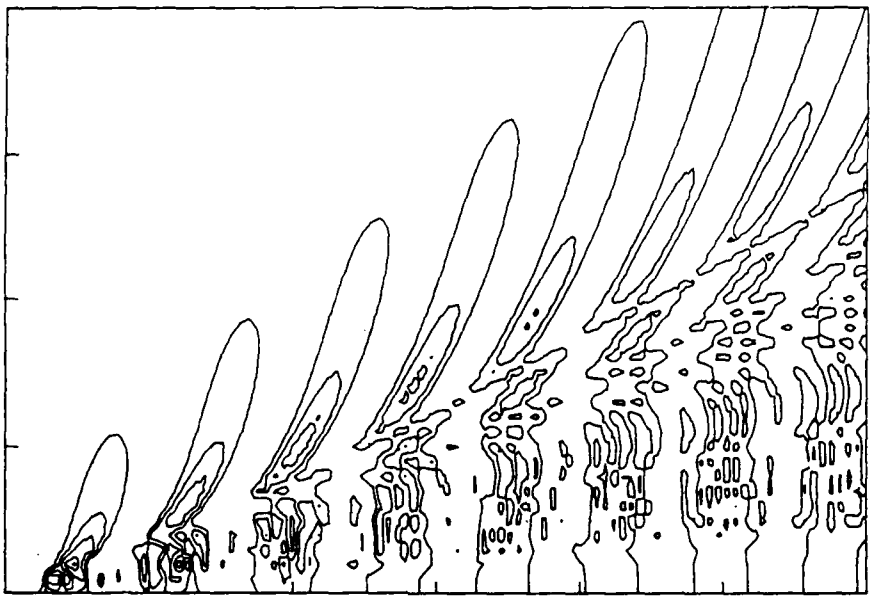

Fig. 6(a) — $z = 0.01$

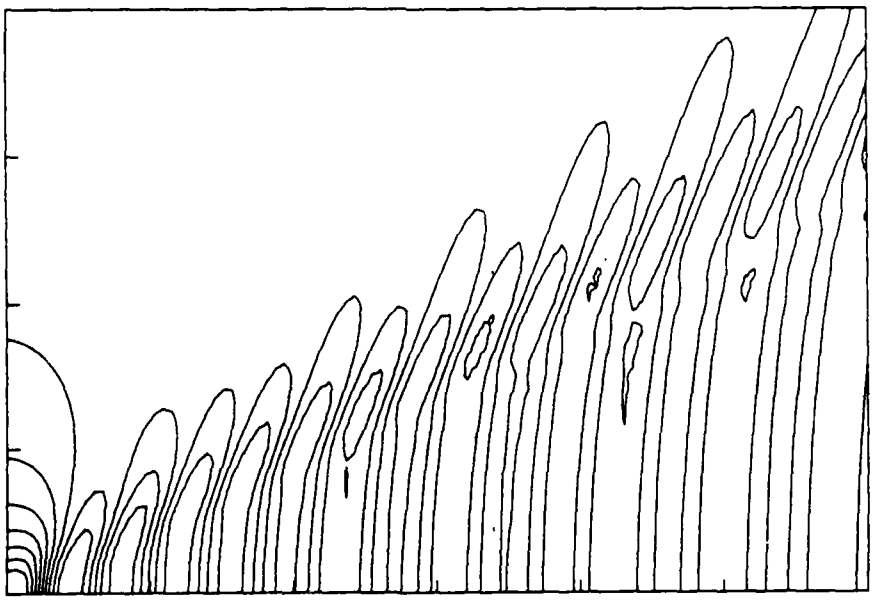

Fig. 6(b) — $z = 1.0$

Fig. 6 — Contour plots of G_e

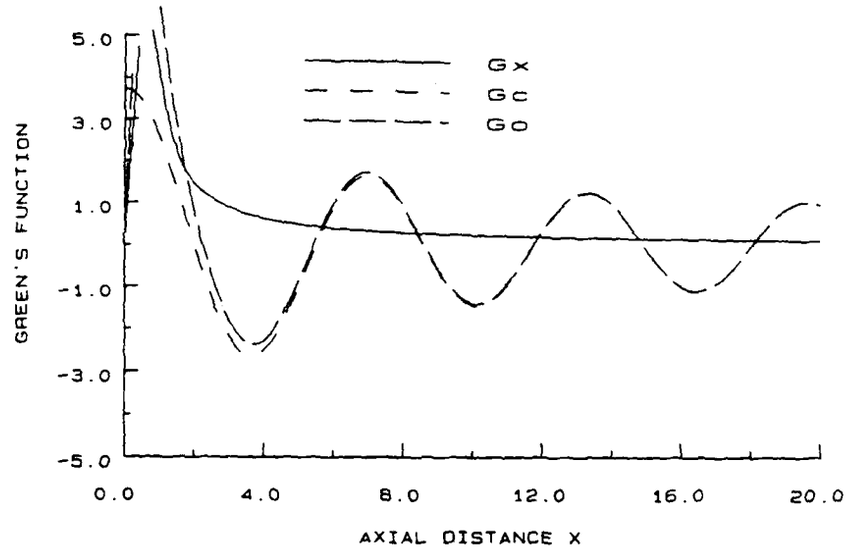

Fig. 7(a) — $y = 0$

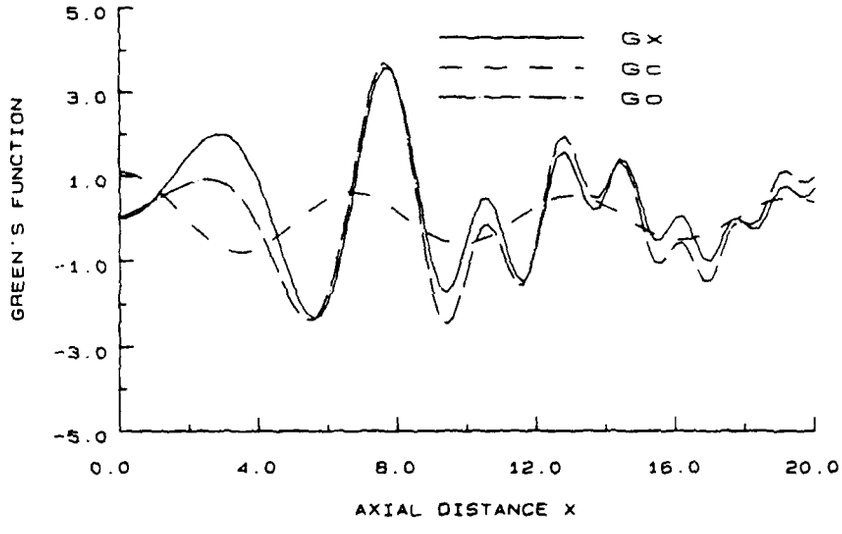

Fig. 7(b) — $y = 2$

Fig. 7 — Line plots of component integrals, $z = 0.1$

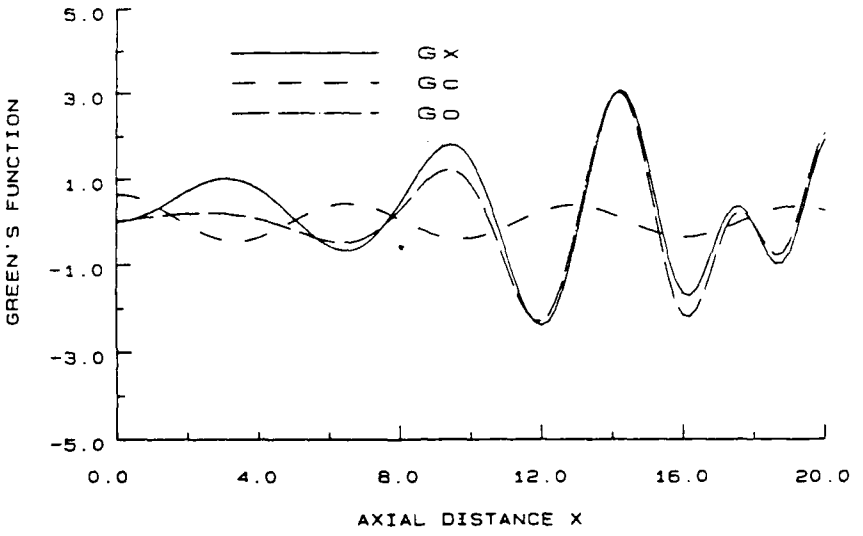

Fig. 7(c) — $y = 4$

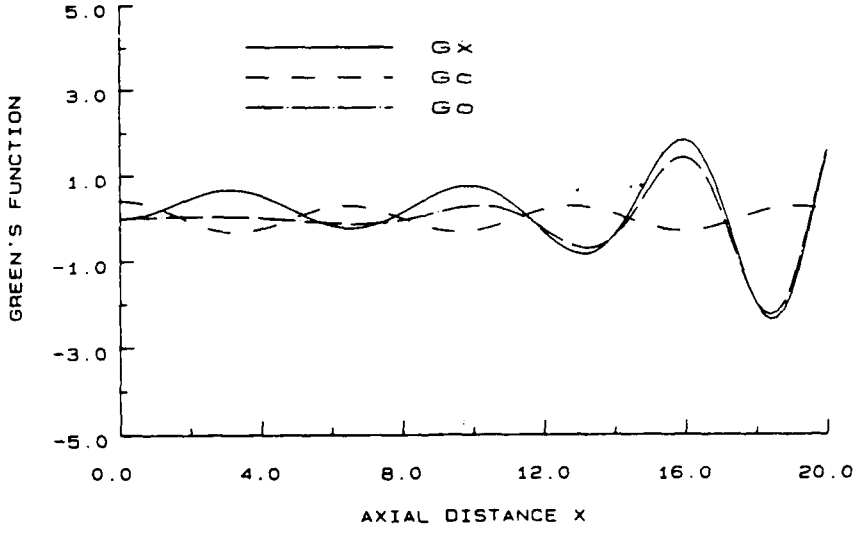

Fig. 7(d) — $y = 6$

Fig. 7 — (Continued) Line plots of component integrals, $z = 0.1$

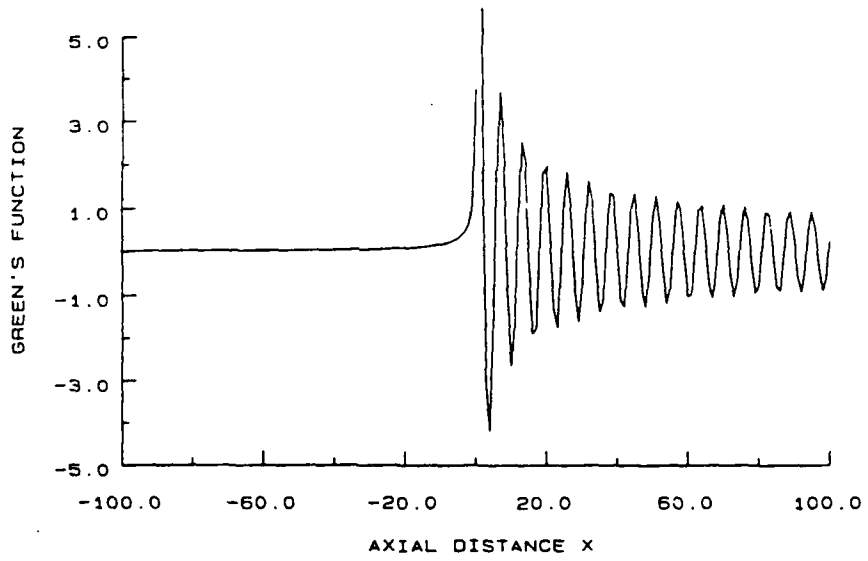

Fig. 8(a) — $y = 0$

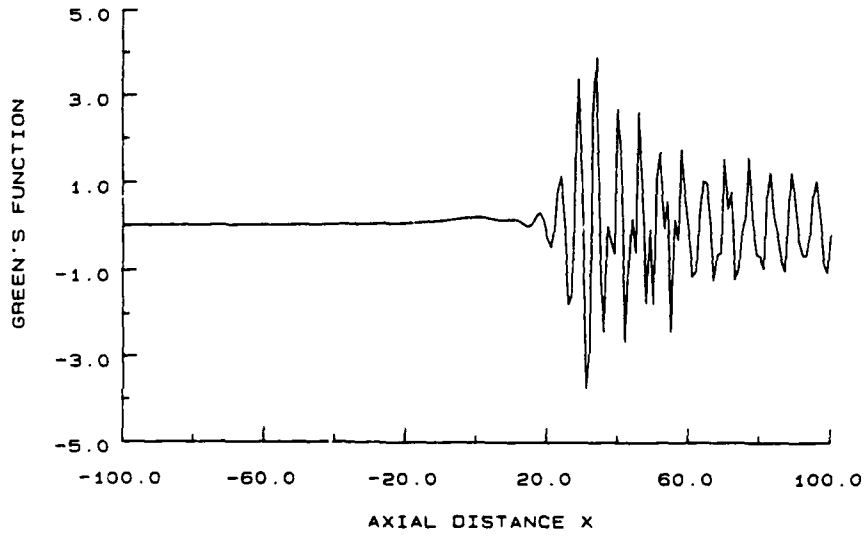

Fig. 8(b) — $y = 10$

Fig. 8 — Upstream and downstream line plots of G_0, $z = 0.1$